

Document downloaded from:

<http://hdl.handle.net/10251/183671>

This paper must be cited as:

Floris, I.; Adam, JM.; Calderón García, PA.; Sales Maicas, S. (2021). Fiber Optic Shape Sensors: A comprehensive review. *Optics and Lasers in Engineering*. 139:1-17.
<https://doi.org/10.1016/j.optlaseng.2020.106508>



The final publication is available at

<https://doi.org/10.1016/j.optlaseng.2020.106508>

Copyright Elsevier

Additional Information

Fiber Optic Shape Sensors: A comprehensive review

Ignazio Floris^{a,b}, Jose M. Adam^{b*}, Pedro A. Calderón^b, Salvador Sales^a

^aITEAM, Universitat Politècnica de València, Camino de Vera s/n, Valencia, 46022, Spain

^bICITECH, Universitat Politècnica de València, Camino de Vera s/n, Valencia, 46022, Spain

Abstract

Fiber Optic Shape Sensing is an innovative Optical Fiber Sensing Technology that uses a fiber optic cable to continuously track the 3D shape and position of a dynamic object (with unknown motion) in real-time without visual contact. This technology offers a valid alternative to existing shape sensing methods, thanks to a combination of advantages (including ease of installation, intrinsic safety, compactness, flexibility, electrically passive operation, resistance to harsh environments and corrosion, no need for proximity or computational or numerical models to reconstruct shape) that can bring remarkable improvements to the fields of Civil, Mechanical and Aerospace Engineering, Biomedicine and Medicine. A considerable research effort has been dedicated to this subject in the last twenty years.

This paper presents an ambitious review of the current state of the art of Fiber Optic Shape Sensors (FOSS) based on Optical Multicore Fibers (MCF) or multiple optical single-core fibers with embedded strain sensors and provides a comprehensive analysis of a wide range of aspects, comprising: (1) existing alternative technologies; (2) an overview of optical fiber sensors (3) characteristics and advantages of fiber optic shape sensors; (4) historical achievements; (4) performance and error analysis; (5) applications; and (6) present and future perspectives.

Keywords: *Fiber-Optic Shape Sensor; Optical Curvature Sensing; Optical Fiber Sensor; Fiber Bragg Grating; Distributed Sensing; Optical Multicore Fiber*

1. Introduction

Fiber optic shape sensing has recently captured the attention of academia and industry and has been investigated by research groups worldwide. This outstanding technology enables the remote 3D shape reconstruction of dynamic objects in real-time in the absence of visual contact. A Fiber Optic Shape Sensor (FOSS) can be defined as fiber optic cable with multiple cores and embedded strain sensors. The working principle is the following: in each instrumented section the three-dimensional curvature is calculated through the simultaneous measurement of strain in different cores. The longitudinal curvature function is determined from the values of strain sensed in the instrumented sections by means of interpolation or curve fitting, while the shape is reconstructed through numerical integration of the curvature.

The great interest of this technology is due to its remarkable potential in a multitude of applications fields, such as Civil, Mechanical and Aerospace Engineering, Biomedicine and Medicine and its improvement over existing methods. Several alternative technologies can be employed for shape reconstruction, such as electrical strain sensors [1–3], accelerometers [4–12], optoelectronic sensors [13,14], electro-mechanical systems based on tilt sensors [15–18], cameras [19,20], RADAR Detection And Ranging (RADAR) [21–23] and laser scanners [24]. Nevertheless, optical fiber shape sensors are significantly more competitive, thanks to the numerous advantages of Optical Fiber Sensor (OFS) technologies [25–32], including: compactness, small size, flexibility, intrinsic safety, resistance to harsh environments and corrosion, and their multiplexing and embedding

* Corresponding author.

E-mail address: joadmar@upv.es (J.M. Adam)

43 capability.

44 FOSS can be classified into two main categories: (I) shape sensors based on optical multicore fibers
45 (a single fiber with multiple cores) and (II) shape sensors based on multiple optical single-core
46 fibers. In this last case, the sensor is composed of several fibers attached to a support, for instance
47 a tube or a bar. The first option ensures compactness, monolithicity (no need for sensor assembly,
48 being manufactured as a single piece), flexibility and small size. The second alternative has higher
49 resolution thanks to the greater core spacing, the distance between the outer cores and the sensor's
50 axis. Other classifications can be made considering the number of cores or the technology employed
51 to sense strain, e.g. Fiber Bragg Grating (FBG), Rayleigh scattering or Brillouin scattering.

52 The objective of this paper is to conduct a multiple-perspective review of the main recent advances
53 in fiber optic shape sensing and aspires to be an exhaustive guide for anyone interested in entering
54 this field of study and a valid support for the experts looking for a thoroughly up-to-date view of
55 the state-of-the-art of this topic.

56 Although other authors have provided an admirable review of patents and research papers on fiber
57 optic shape sensors [33], the present review is probably the most ambitious so far as it takes into
58 account a wide range of aspects, comprising:

- 59 • An analysis of the existing technologies used to reconstruct shape, with particular attention
60 to characteristics, advantages and disadvantages (Section 2);
- 61 • A concise overview of optical fiber sensors (Section 3)
- 62 • An extensive description of fiber optic shape sensors, considering characteristics,
63 classification and advantages and a special focus on the strain sensing technologies used
64 (Section 4);
- 65 • A bibliographic review of the historical achievements and the recent developments of fiber
66 optic curvature, twisting and shape sensing (Section 5);
- 67 • An examination of the performance and error analyses conducted (Section 6);
- 68 • A summary of the applications in which these sensors have been used or have potential to
69 be implemented (Section 7);
- 70 • The authors' considerations on present and future perspectives (Section 8).

71 **2. Existing technologies for shape sensing**

72 Shape measurement plays an important role in the fields of Civil, Mechanical and Aerospace
73 Engineering, Biomedicine and Medicine, for applications such as the structural health monitoring
74 of civil structures and infrastructures (buildings, tunnels, bridges and roads), reconstruction of the
75 displacement field of critical components (wings and aircraft) and tracking robots and medical
76 instruments (needles, catheters endoscopes) inside the human body. For the foregoing reasons,
77 many researchers and industries have developed several shape reconstruction methods exploiting
78 diverse technologies, including:

- 79 ➤ Shape sensing based on electrical strain sensors [1–3];
- 80 ➤ Vibration-based shape sensing using accelerometers [4–12] ;
- 81 ➤ Monitoring systems consisting of acquisition devices, computers, and processing software
82 able to reconstruct shape using data collected by cameras [19,20,34], radio detection and
83 ranging (RADAR) [21–23] or laser scanner [24,35,36];
- 84 ➤ Electro-mechanical sensing systems that reconstruct shape by measuring angles with tilt
85 sensors [37], such as inclinometers [15–18];
- 86 ➤ Optoelectronic shape sensing [13,14].

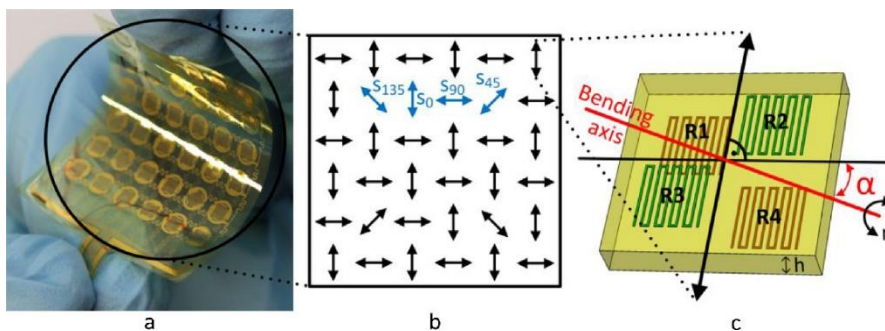
87 This section reviews the existing methods available in the market capable of performing shape
88 sensing, classified according to the technology used.

89 2.1. Strain sensors

90 Electrical strain gauges are one of the most widely used devices to measure strain [38,39]. The
 91 sensing principle is simple: strain gauges are electrical conductors and when attached to the object
 92 to be monitored deform together with it. This deformation produces a change in the electrical
 93 resistance through which it is possible to calculate the strain to which the object is subject. Optical
 94 fiber sensors have also been broadly used for this purpose [40–42], as will be better illustrated in
 95 Section 4.3. However, it has to be pointed out that fiber-optic strain sensors are completely different
 96 from FOSS, since they only measure strain.

97 Strain sensors have been intensively employed in Structural Health Monitoring (SHM) [43] for
 98 several purposes, including damage detection [44], structural fatigue life evaluation [45] and
 99 deformation monitoring [3]. In this last case, firstly, a Finite Element Model (FEM) of the structure
 100 under examination is developed. Then a series of points of measurements are selected and the strain
 101 gauges are installed in these locations. Finally, the values of strain detected are used as inputs for
 102 the FEM and the deformed shape of the structure is determined. This technique has some
 103 disadvantages: the installation of the sensors can be costly, the development of complex models is
 104 eminently time-consuming and significant approximations are required to interpret the structure
 105 behavior from the limited number of measurement points considered [45].

106 An alternative method of shape sensing consists of flexible sensor systems based on electrical strain
 107 gauges. Koch et al. designed and tested a small and ultra-thin flat polyimide foil with 36 bending
 108 measurement points, illustrated in Fig. 1, able to reconstruct the shape of surfaces on the basis of
 109 bending measurements [1]. This technology can reconstruct shape directly without the development
 110 of models but unfortunately the modest size of the sensor limits its scope of applications.
 111



112

113 **Fig. 1.** (a) Hand-bended 6 × 6 bending sensor instrumented foil. (b) Illustration of sensors orientations. (c)
 114 Illustration of the sensor under bending [1].

115 2.2. Accelerometers

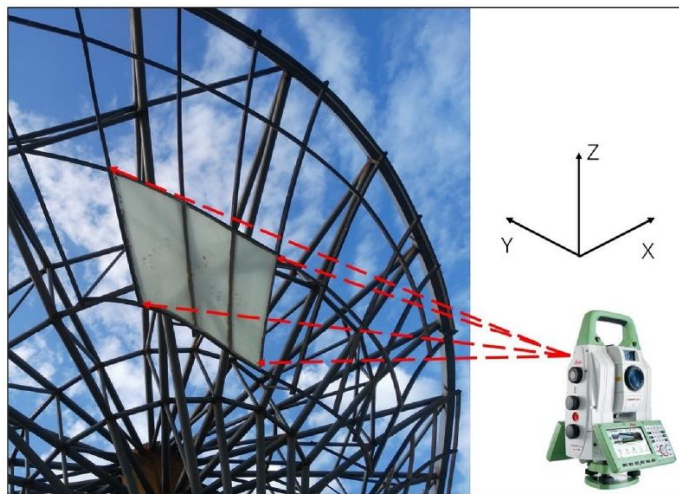
116 Accelerometers are able to measure the acceleration (rate of change of the velocity) of an object.
 117 Several systems based on accelerometers have been proposed for direct shape sensing [8–12],
 118 whose main applications are the analysis of human motions and spine shape monitoring. These
 119 systems are constituted by a series of sensor nodes, instrumented with electrical accelerometers
 120 rigidly connected to each other and track the shape by means of complex reconstruction algorithms.
 121 Regrettably, the range of application of these systems is notably reduced by their limited embedding
 122 capability.

123 Accelerometer-based methods are broadly used in structural health monitoring for damage detection
 124 in civil and mechanical structures through mode shape identification [46,47] and permit the
 125 understanding of the global structural behavior, considering an extremely limited number of
 126 measurement points, conveniently selected [4,5,48]. First, the mode shapes of the structure are
 127 identified by means of the accelerometers attached to the structure [4,5,49]. Two different damage

128 detection approaches can then be employed to assess the structural integrity: model-based and data-
129 based. Model-based methods consist of the comparison of the measured structural response with
130 predictions resulting from computational models of the analyzed structure [6]. The presence of
131 damage in the structure, as well as its location and severity assessment, can be determined from the
132 differences between predicted and measured data [44]. The main limitation of these methods is that
133 the development of accurate computational models is not always easy and sometimes not even
134 possible. Data-based approaches rely on pattern recognition algorithms and compare data obtained
135 from the intact and damaged structure [50]. The principal limitations of these approaches are that
136 the data of one or more damaged conditions are generally not available *a priori* and in the case of
137 existing structures even the data from the intact structure are often not available.

138 2.3. Monitoring systems based on cameras, RADAR or laser scanner

139 Vision-based approaches are widely used in industrial robotics [51] for robot motion tracking and
140 in civil engineering to monitor the deformation of civil structures and infrastructure and assess their
141 integrity, offering a noncontact alternative to the employment of sensors [19,20,34]. A vision-based
142 measurement system consists of image acquisition devices, computers, and an image processing
143 software. The data collected from cameras are processed with specific numerical algorithms to track
144 motions, obtain the mechanical parameters for structural monitoring, detect visual abnormalities
145 and extract the time histories of displacement, deformation and shape. Image processing techniques
146 suffer from a series of limitations [52]: inability to carry out in-field continuous monitoring due to
147 complicated site conditions and infrastructure closure during the data acquisition. When high speed
148 data acquisition is not necessary, in addition to camera-based methods, radio detection and ranging
149 (RADAR) and laser scanner can be used in structural health monitoring [21–24,35,36]. Laser
150 scanners are particularly useful to track 3D shape (see Fig. 2), while RADAR allows the
151 deformation tracking of large structures even if with less accuracy than cameras.
152



153

154 **Fig. 2.** Three-dimensional shape/position tracking of a civil structure using 3D laser scanning [36].

155 2.4. Electro-mechanical systems based on tilt sensors

156 Electro-mechanical systems based on tilt (or slope) sensors, mainly known as inclinometers, are
157 used to reconstruct three-dimensional shape based on the measurement of angles [15–18]. These
158 instruments are commonly employed in health monitoring of structures and infrastructures
159 [16,18,53] and geotechnical applications [17], where they are used to measure horizontal

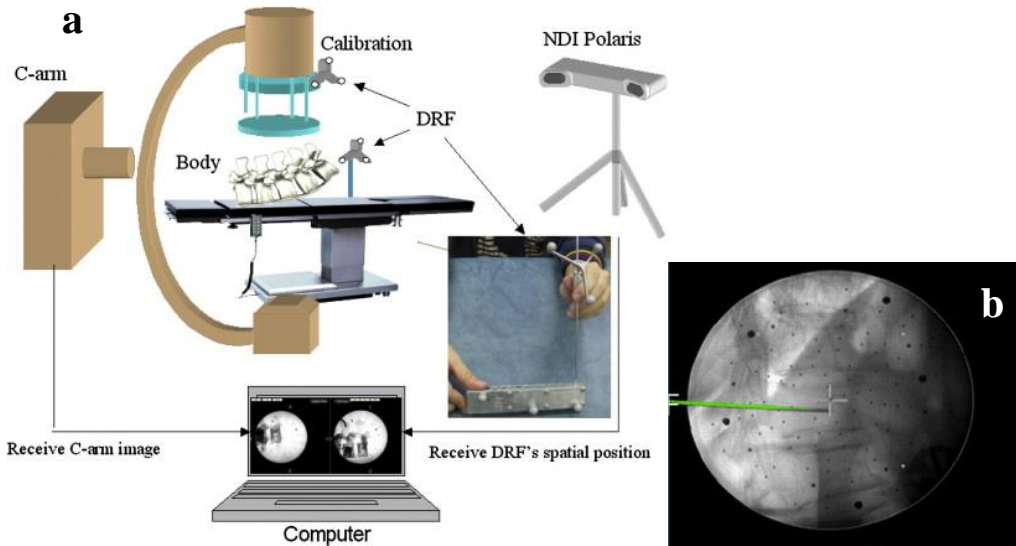
160 displacements at various points of a borehole (slope inclinometers). An inclinometer measurement
161 system is a combination of components: a grooved casing, which can be attached to the structure or
162 installed in a borehole, inclinometer probe and data acquisition equipment. The inclinometer probe
163 is manually moved along the length of the casing to measure angles in two perpendicular planes by
164 means of accelerometers or gyroscopes. Unfortunately, this operation requires time and monitoring
165 personnel to obtain a series of measurements. Alternatively, a fixed In-Place-Inclinometer (IRI) can
166 be employed to collect data continuously [53]. An IRI is composed of a sequence of wheeled probes
167 connected to each other through extension rods. The probes do not need to be manually moved and
168 can operate continuously, saving time and labor. The deformation of structures or the displacement
169 fields of slopes or landslides can be reconstructed from the angles measured at various depths along
170 the casing. The most significant advantages of these sensors are: their great length, generally tens
171 of meters, and accuracy, for instance servo-accelerator probes, which have the highest resolution
172 of the available inclinometers on the market, reach a maximum system precision of 1.2 mm per 30
173 m or 1:24,000, while the usual precision is six times lower without corrections for systematic errors
174 [53]. The principal disadvantages are the low speed data acquisition and the continuous exposure
175 of the system to corrosion in the case of in-place-inclinometers.

176 2.5. *Optoelectronic sensors*

177 Optoelectronics shape sensors are hybrid systems capable of tracking the shape of an object in real-
178 time, using a combination of light and electrical sensors, such as gyroscopes and accelerometers,
179 and mirrors [14,54,55]. The sensors that belong to this category are very diverse and rely on
180 different operating principles and sensing technology, therefore, is not possible to give a simple
181 definition and a description of their characteristics.

182 2.6. *Fluoroscopy*

183 Fluoroscopy is an imaging technique that provides real-time feedback of position and shape of
184 surgical instrument inside the human body using X-rays [56]. This technology finds application in
185 a number of image-guided procedures, such as orthopedic and spine surgery [57,58], cardiac
186 interventions [59], epidural injections [60] and cervical pedicle screw insertion [61]. The
187 fluoroscopic navigation procedure consists of 4 basic steps [62]: (I) reference array attachment to
188 the skeleton of the patient to enable tracking during the operation; (II) image acquisition by means
189 of the fluoroscope and transfer to the computer workstation; (III) calibration to improve and sharpen
190 fluoroscopic images; (IV) superimposition of the predicted shape and position of the medical tool
191 onto the harvested image. Fig. 3 shows a fluoroscopy-based C-arm setup and an example of X-ray
192 image tracking a vertebroplasty cannula.



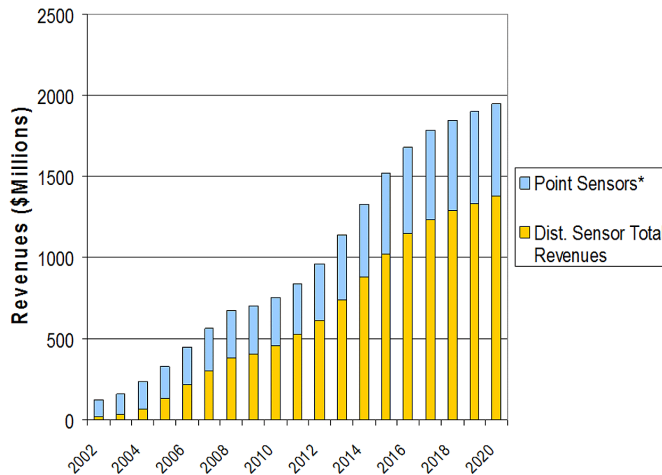
193

194 **Fig. 3.** (a) Setup configuration of the C-arm image-guided. (b) Position of a vertebroplasty cannula displayed
 195 and tracked using computer image and fluoroscopy image [63].

196 Fluoroscopy is widely used to ensure minimally invasive medical procedures, thanks to its
 197 fundamental advantages: no need for visual contact and real-time measurements. Nonetheless, this
 198 technology presents several drawback, including high cost, bulkiness, low-speed data acquisition
 199 and above all prolonged patient exposure to radiation [57,58].

200 **3. Optical Fiber Sensors**

201 Optical Fiber Sensors (OFS) have undergone considerable expansion over the last few decades (see
 202 Fig. 4) in several different fields [64], such as the engineering [65,66], industrial [67], medical [68],
 203 chemical [69,70] and biological [71,72].
 204



205

206 **Fig. 4.** Point sensor and distributed sensor market revenue and forecast, 2002–2020. Sources: historical data
 207 from Light Wave Ventures, OIDA forecast from member input. Courtesy of OIDA.

208 The principal reasons behind this substantial growth are their inherent ability to sense a variety of
209 measurands (as defined by [73]) in continuous development [74], such as strain [75,76], temperature
210 [70], moisture [77], vibrations [78], chemical agents [72], and many others [37], using the optical
211 fiber itself as a sensor. OFSSs have considerable advantages over their electrical counterparts,
212 comprising [25–32]:

- 213 ➤ Compactness, small size and lightweight;
- 214 ➤ Flexibility;
- 215 ➤ Monolithicity (no need for assembly, being manufactured as a single piece);
- 216 ➤ Electrically passive operation;
- 217 ➤ Resistance to harsh environments, including humidity, severe temperature, chemicals and
218 radiation;
- 219 ➤ Immunity to Electromagnetic Interference (EMI);
- 220 ➤ Corrosion resistance;
- 221 ➤ Embedding capability;
- 222 ➤ Multiplexing capability;
- 223 ➤ Intrinsic safety (no electricity required in the sensor);
- 224 ➤ High sensitivity and accuracy;
- 225 ➤ Multiparameter sensing capability [74].

226 The large majority of optical fibers are made of silica (drawing glass), a material with extraordinary
227 characteristics. Silica has high mechanical tensile and even flexural strength as well as high
228 flexibility and almost perfect elastic behavior. Silica is chemically stable and practically inert [79–
229 82]. The process of optical fiber manufacturing, fiber drawing, developed to provide high speed and
230 high performance data transmission for communication applications, requires extremely high
231 accuracy and specialization. A preformed tip is heated, and then the optical fiber is pulled out in an
232 apparatus known as a draw tower. The combination of the exceptional characteristics of silica and
233 the extremely advanced drawing process guarantees optical fiber sensors these unique properties
234 for sensing purposes. The multiplexing capability, which is the ability to multiplex a multitude of
235 optical sensors on one single fiber and monitor them by a single remote interrogator unit, provides
236 a notable advantage to this technology for sensing applications over the shape sensing alternatives.

237 **4. Shape sensing based on Optical Fiber Sensors**

238 One of the current frontiers of the fiber-optic sensing technologies is shape sensing [33], which
239 consists of the ability to dynamically track position and shape of any point on an optical fiber cable
240 in three-dimensional space. Fiber optic shape sensors are optical Multicore Fibers (MCF) or multi-
241 fiber cables (with a similar section geometry to MCFs, but larger core spacing) capable of sensing
242 multidimensional curvature along the sensor's length by comparing the longitudinal strain detected
243 in different cores and reconstructing the shape [83]. This innovative technology has been an area of
244 great interest for many researchers by reason of its great potential for a number of industrial and
245 medical applications that require curvature, twisting and 2D/3D shape sensing.

246 **4.1. Advantages**

247 The existing shape sensing methods present several limitations, in particular the necessity for
248 complex numerical algorithms or computational models for data analysis and shape reconstruction.
249 Shape sensing is particularly critical in applications that require the tracking of a dynamic object in
250 the absence of visual contact. FOSSs offer an extremely valid alternative to traditional methods,
251 allowing the shape to be tracked continuously, dynamically directly and without the need for visual
252 contact or models. As shape sensors need to be attached to the object to be monitored, compactness
253 and small size, flexibility and embedding capability, peculiar characteristics of optical fiber sensors,
254 guarantee ease of installation and efficient shape tracking. Ultimately, immunity to electromagnetic

255 interference, resistance to harsh environments and corrosion and high sensitivity and accuracy make
256 this technology suitable for a wide range of applications. The principal advantages of fiber optic
257 shape sensing can be summed up as follows:

258

259 I) Ability to sense the shape of an object directly, without computational and numerical
260 models and with no necessity for approximations, such as assumptions about the
261 characteristics of structures or soil (mass, stiffness, mechanical properties) in SHM
262 applications;

263 II) Ease of installation, the sensor being a single cable;

264 III) No necessity for visual contact;

265 IV) Capability of continuous, dynamic, real-time and durable monitoring, especially
266 convenient for structural health monitoring and industrial robotics applications;

267 V) All the advantages of optical fiber sensor technologies.

268 4.2. FOSS section characteristics

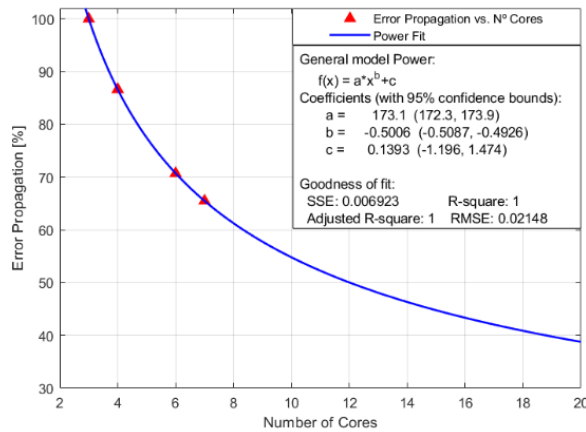
269 The section geometry as well as the number of cores and configuration of a fiber optic shape sensor
270 have notable impact on its accuracy in sensing curvature [84,85], twisting [86] and shape [83] and
271 on its embedding capability. Considering a FOSS subject to bending, the curvature induces a
272 longitudinal strain in the outer cores proportional to their distance from the neutral axis, according
273 to the Euler-Bernoulli-Saint-Venant beam theory [87–89]. Consequently, at equal values of
274 curvature, the strain generated in the outer cores increases with greater core spacing, the distance
275 between the sensor axis and the outer cores, enhancing the sensor's sensitivity to curvature. Similar
276 considerations can be made in the case of twisting [86]. The increased core spacing requires a larger
277 diameter of the section, reducing the embedding capability of the sensor, due to the greater
278 dimensions. In view of the foregoing, the most appropriate section geometry depends on the
279 application and on the specific characteristics needed. Two different categories of FOSSs have been
280 investigated in the literature: MCF-based [83,86,90–94] and multi-fiber-based [95–100].

281 The first typology implements optical multicore fibers, a special fiber with multiple cores embedded
282 in a common cladding. The multiple cores make the fiber sensitive to curvature (and potentially to
283 twisting), in addition to longitudinal strain. Unfortunately, the MCFs available in the market and
284 suitable for shape sensing applications are limited, since they are usually the same as those
285 manufactured for telecommunication applications. Normally, their cladding diameter is extremely
286 small (around 125 μm) and the core spacing is between 30 and 50 μm [92–94,101–104]. The
287 manufacture of different and customized MCF geometries for sensing applications would be
288 extremely expensive, as the sensor market is modest compared to telecommunications. In the light
289 of the above, ordinarily MCF-based FOSSs have small core spacing, but offer the following
290 advantages: monolithicity, compactness, flexibility, small size, high embedding capability and high
291 manufacturing accuracy, being manufactured through the extremely advanced drawing process of
292 optical fibers.

293 The FOSSs belonging to the second category are constituted of fiber bundles, several optical single-
294 core fibers epoxy-molded [100] or fastened to a support, such as a tube or a bar [95,99]. This
295 configuration guarantees a remarkably larger core spacing and consequently higher curvature
296 resolution and enhanced accuracy in curvature, twisting and shape sensing. The fibers can be
297 interrogated without the need for a fan-in/out, as in the case of MCF-based FOSSs. In contrast,
298 multi-fiber-based FOSSs require to be assembled and the wide section limits their embedding
299 capability.

300 Depending on the application, one or the other variant is the most fit for purpose. For instance, in
301 the case of medical instruments, such as needles and catheters, small size, compactness and high
302 embedding capability are essential features to ensure easy insertion into the human body. Whereas
303 the FOSSs used in geotechnical applications or structural health monitoring require extremely high

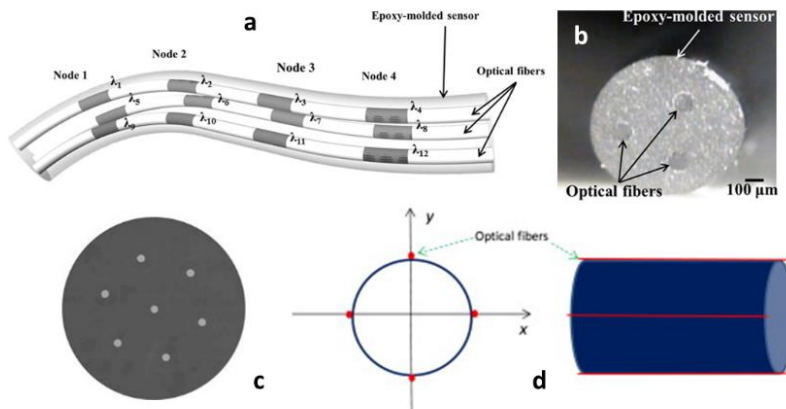
304 accuracy in shape reconstruction to detect ground movements, due to the small displacement
 305 magnitude, or track the shape deformation of structures because of the modest structural
 306 deformability of these elements.
 307 Under the beam theory, three nonaligned measurement points in each instrumented section of a
 308 FOSS are sufficient to sense three-dimensional curvature [83–85,93]. In addition to three outer
 309 cores, the presence of a central core also allows the twisting to be sensed by comparing the
 310 longitudinal strain of outer and central cores [86,105]. Nevertheless, additional cores can be
 311 employed to ensure measurement redundancy [106] and improve the accuracy, as shown in Fig. 5.
 312 Overall, the FOSSs currently adopted have very diverse section geometries with different core
 313 spacing and number and configuration of cores; the most widely utilized are the three- [93,96], four-
 314 [94,97,107] and seven-core section [91,92,108–111], with constant angular spacing and core
 315 spacing, as illustrated in Fig. 6.



316

317

Fig. 5. Representation of the effects of core position errors as a function of number of cores [85].



318

319

320

321

Fig. 6. Example of FOSSs: epoxy-molded three-core shape sensor [100], (a) three-dimensional view and (b) cross-section; (c) seven-core multicore fiber cross-section [112]; (d) optical four-core fiber inclinometer tube [113].

322 4.3. Strain sensing technologies

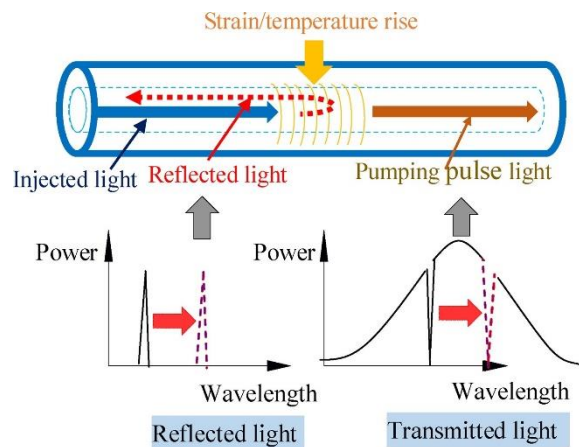
323 The process of shape tracking is divided into three phases: strain sensing, curvature calculation and
 324 shape reconstruction. It is hence evident that the technology employed to sense strain, being at the
 325 basis of the process, strongly influences FOSS performance. The strain sensing technologies most
 326 commonly used in fiber optic shape sensing are here briefly reviewed.

327 4.3.1. Fiber Bragg Grating

328 Fiber Bragg Gratings (FBG) are Bragg reflectors, well-established as highly sensitive strain and
 329 temperature single-point sensors (quasi-distributed sensing) [26,114]. FBGs are the most widely
 330 used optical fiber sensors and have a multitude of engineering applications [115–122]. One of the
 331 most significant advantages of these sensors is the ability to perform dynamic strain sensing, thanks
 332 to their high frequency data acquisition (~ kHz).

333 FBGs are constructed by laterally exposing the core of an optical fiber to an intense laser light with
 334 a periodic pattern [123,124]. The exposure permanently increases the refractive index of the core.
 335 This fixed index modulation is a grating and has a period that depends on the exposure pattern. A
 336 fiber Bragg grating allows the transmission of some wavelengths and reflects others (see Fig. 7),
 337 corresponding to the FBG wavelength peak, which is related to its period. Since the period of a
 338 grating varies with temperature and longitudinal strain, it is possible to sense these quantities by
 339 tracking the grating wavelength peak.

340



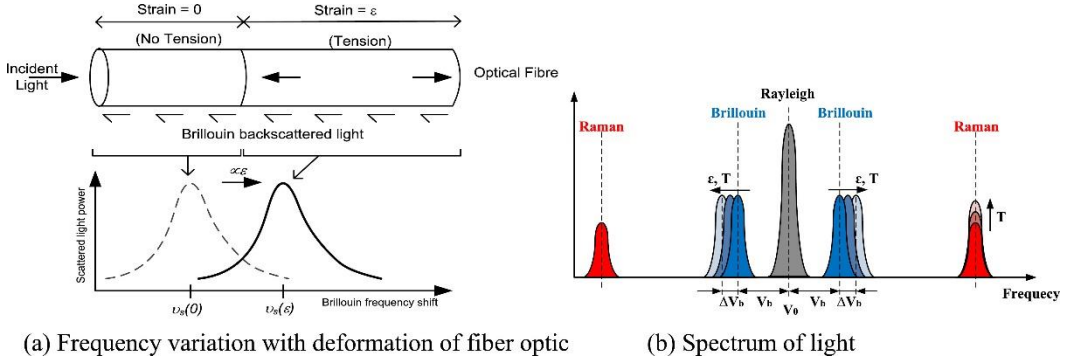
341

342 **Fig. 7.** Sensing principle of fiber Bragg grating sensor [125].

343 4.3.2. Distributed sensing

344 Light scattering is caused by the interaction between the atoms or molecules of a medium and the
 345 incident electromagnetic (EM) waves that pass through it and consist of absorption of energy and
 346 its re-emission in different directions at various intensities. Light scatters through three different
 347 processes (illustrated in Fig. 8): Raman (sensitive to temperature), Brillouin (sensitive to both
 348 temperature and strain), and Rayleigh (sensitive to strain).

349



350 (a) Frequency variation with deformation of fiber optic

(b) Spectrum of light

351 **Fig. 8.** Principals of distributed optical fiber sensing [126].

352 Only Rayleigh and Brillouin scattering are able to sense the strain of the medium. In the 80s, this
 353 loss in propagation was first exploited for the development of distributed sensing configurations
 354 using optical fibers [127]. The idea of distributed sensing consists of a sensing element with linear
 355 geometry and a sensing system able to measure the value of the measurand considered, e. g. strain,
 356 at any position along the sensing element. The performances of Distributed Optical Fiber Sensors
 357 (DOFS) are evaluated by three characteristics that are generally interdependent: the accuracy of the
 358 measured quantity, the sensing length or sensing range (range for the position) and the spatial
 359 resolution (minimum distance to measure variations in the measurand along the optical fiber,
 360 equivalent to the gauge length of a discrete sensor). Compared with FBGs, distributed sensors have
 361 significantly lower frequency data acquisition, which depends on the technology and on the sensing
 362 range (an indicative value could be ~ mHz / Hz). DOFSs have been comprehensively reviewed in
 363 the literature [42,127–130].

364 4.3.3. Distributed sensors based on Rayleigh scattering

365 DOFSs based on Rayleigh scattering are usually classified into two categories: Optical Time
 366 Domain Reflectometry (OTDR) and Optical Frequency Domain Reflectometry (OFDR).

367 An OTDR launches a light laser pulse into an optical fiber. The returning light, Rayleigh
 368 backscattered light, is collected and is fed into the receiver where its optical power is measured as
 369 a function of time (attenuation in the time domain). The evolution of the power over time of the
 370 detected signal provides information of position and magnitude of the quantity to be measured
 371 distributedly along the fiber length [131]. The efficiency of OTDR is very limited when high spatial
 372 resolution (less than one meter) is required, while the common sensing range is around 1/10 km
 373 [42,128,130].

374 OFDR systems have attracted the interest of many researchers driven by the necessity for short
 375 spatial resolutions (millimeter scale) and cost effective distributed optical fiber sensors. On the other
 376 hand, the sensing range of this technique is notably less than OTDR and, commonly in the range of
 377 10/35m [42,128,130]. OFDR operates in the frequency domain (or Fourier domain): an OFDR
 378 sensor system tunes a frequency range and receives a frequency response from the optical fiber
 379 which is converted into the time/spatial domain by Fourier transform.

380 Optical frequency domain reflectometry exists in two variants: Incoherent OFDR (I-OFDR) and
 381 Coherent OFDR. The main difference is that in I-OFDR the source is not pulsed, but generates CW
 382 light by modulating the optical intensity with radio frequency (RF) signals. While in the case of
 383 Coherent OFDR the source is obtained by sweeping the optical frequency [131].

384 OFDR Rayleigh sensing can be performed simply by utilizing the inherent Rayleigh scattering from
 385 the core of the fiber. Otherwise, in order to increase the sensitivity in distributed strain sensing, the
 386 Rayleigh signal strength can be enhanced by exposing the optical fiber to ultraviolet (UV) laser

387 [132] or inscribing a continuous grating into the cores of the fiber [91,110].

388 4.3.4. Distributed sensors based on Brillouin scattering

389 The most significant distributed optical fiber sensing techniques based on Brillouin scattering are:
 390 Brillouin Optical Time Domain Reflectometry (BOTDR) and Brillouin Optical Time Domain
 391 Analysis (BOTDA).

392 BOTDR refers to the time domain interrogation of spontaneous back-propagating Brillouin
 393 scattering. The concept is analogous to the OTDR used in Rayleigh backscattering, but, in this case,
 394 the spatial resolution is in the range of 1 meter/tens of meters and the sensing range is up to tens of
 395 kilometers [42,128,133].

396 BOTDA has a more elaborate form than BOTDR and is based on Stimulated Brillouin Scattering
 397 (SBS). The BOTDA technique consists of the launch, from both the extremities of optical fiber, of
 398 an intense pulse and Continuous Wave (CW) light with a frequency difference equivalent to the
 399 Brillouin frequency shift [42,134]. The intense pump pulse interacts locally during its propagation
 400 with the weak CW probe and the gain obtained by the probe at each location along the fiber length
 401 can be determined by analyzing the probe amplitude in the time domain. This stimulated scattering
 402 process produces a more intense Brillouin scattering that requires less averaging to achieve a
 403 reasonable Signal to Noise Ratio (SNR) of the system.

404 **5. Historical achievements in fiber optical shape sensing**

405 This section reviews the principal achievements regarding fiber optic curvature, shape and twisting
 406 sensing present in the literature, briefly summarized in Table 2.1.

407 **Table 1.** Historical progress in fiber optical shape sensing.

Starting year	Contribution	Description	Refs.
1980s	Optical fiber strain sensors	Demonstration of distributed and quasi-distributed strain and temperature sensing using optical fibers.	[114,135]
1980s	Multiplexing technique	The development of multiplexing techniques to interrogate several Bragg grating sensors on a common fiber path enabled quasi-distributed measurements of strain and temperature.	[136–138]
~ 1998	MCF-based interferometric bending sensor	The employment of optical multicore fiber enabled the measurement of degree and orientation of bending by comparing the strain in a pair of cores, using interferometric interrogation.	[139–142]
~ 2000	Bending sensor using FBGs	Curvature measurements were demonstrated by using fiber Bragg gratings. The gratings were written into separate cores of a multicore fiber and acted as independent, but isothermal, strain gauges, providing a temperature-independent measurement of the local curvature.	[143]
~ 2003	3D bend sensor	By employing three or more non-aligned strain sensors inscribed into the cores of an optical multicore fiber section, it was possible to measure the local three-dimensional curvature (curvature magnitude and bending direction).	[94,144,145]
~ 2004	2D and 3D shape sensor	Shape sensing was enabled thanks to the development of approaches for shape reconstruction of optical fiber cables with embedded FBGs, by integrating the curvature sensed	[146–148]

		along the sensor and aligning successive arc segments of fixed curvature.	
~ 2007	Shape sensor using OFDR	Optical Frequency Domain Reflectometry (OFDR) technique permitted distributed shape sensing based on Rayleigh scattering using an optical multicore fiber.	[149,150]
~ 2012	Novel method for 3D shape sensing	An innovative method, based on the numerical resolution of a set of Frenet-Serret equations, was proposed to reconstruct complex three-dimensional fiber shapes as a continuous parametric solution, instead of sequence of arcs.	[93,151].
~ 2014	Twisted seven-core multicore fiber	Optical twisted multicore fibers for sensing applications were designed and manufactured to enable twisting compensation in shape sensing, since the use of twisted MCF increases the sensitivity to twisting.	[86,91,92,108,112,152]
~ 2014	Continuous gratings in multicore fiber	An inscription apparatus and a fabrication scheme that allow the continuous inscription of gratings over meters in all cores of multicore fiber through UV transparent coating were proposed. Continuous gratings increase signal to noise ratio and shape sensing precision, compared to the bare Rayleigh scattering of the optical fiber without gratings.	[92]
~ 2016	Shape sensor using Brillouin scattering	Distributed shape sensing based on Brillouin scattering was performed using an optical multicore fiber and a Brillouin optical time-domain analyzer.	[109]
~ 2016	Force and shape sensor	A force and shape sensors for medical applications was developed using an optical fiber sensor with embedded FBGs.	[95,153]

408 5.1. Curvature sensing

409 Curvature sensing (also called bending sensing) is the preliminary step for shape reconstruction.
 410 The first achievements in this subject were reached in the 1990s. Greenaway et al. filed an
 411 international patent and an US Patent, in 1998, describing an optical fiber bending sensor based on
 412 MCF able to measure degree and orientation of the bending present along its length [139,140]. In
 413 1999, Blanchard et al. described a novel three-core photonic crystal fiber and demonstrated its
 414 ability to measure bending in two dimensions using interferometric interrogation at a single
 415 wavelength [141]. Gander et al. (2000) first demonstrated curvature measurements by using Bragg
 416 grating inscribed in a multicore fiber [143]. Flockhart et al. in 2003 first demonstrated the use of
 417 fiber Bragg gratings written into three separate cores of a multicore fiber for two-axis curvature
 418 measurement [94]. Clements filed a patent (2003) illustrating a flexible “smart cable” able to
 419 measure the local curvature and torsion along its length [145]. In 2004 MacPherson et al. first
 420 reported on the use of a 4-core multicore fiber incorporating FBG strain sensors in each core as a
 421 fiber optic pitch and roll sensor [144].

422 Before this, the attention of researchers mostly concentrated on the development of curvature point
 423 sensors, by exploiting fiber Bragg grating technology. A few years before, diverse multiplexing
 424 techniques to perform quasi-distributed measurements were established [136]. One of the first
 425 examples of these methods was proposed by Kersey and Morey, in 1993, who described a technique
 426 for the detection of wavelength shifts in wavelength-encoded fiber Bragg grating sensors capable
 427 of interrogating several Bragg grating sensors on a common fiber path using a mode-locked laser
 428 principle [137]. With the advent and diffusion of these techniques, quasi-distributed curvature
 429 sensing was also finally demonstrated. Chen and Sirkis filed a patent (1998) describing a fiber optic
 430 system able to produce multiple strain measurements along one fiber path for determining the shape
 431 of a flexible body, by using Bragg grating sensor technology and time, spatial, and wavelength

432 division multiplexing [138]. Barrera et al. developed a multipoint curvature optical fiber sensor
433 based on a non-twisted homogeneous four-core fiber, using Wavelength Division Multiplexing
434 (WDM) [107]. A novel experimental setup was developed and an array of 15 FBGs was produced
435 and tested by sensing constant curvatures. The sensor was able to sense curvature with high
436 accuracy, obtaining a standard deviation under 1.6% in the applied curvature range.

437 Alternative technologies to fiber Bragg grating were employed to perform fiber optic curvature
438 sensing. Barrera et al. developed a directional curvature sensor based on long period gratings
439 inscribed in a multicore optical 7-core multicore fiber [154].

440 In addition to quasi-distributed curvature sensing by means of FBG technology, distributed
441 curvature sensing has also been performed. Zafeiropoulou et al. measured the curvature of a D-
442 shaped multicore fiber using Brillouin optical time-domain reflectometry [155]. Szostkiewicz et al.
443 distributedly sensed the curvature of an MCF using phase-sensitive Optical Time-Domain
444 Reflectometry (ϕ -OTDR) [156].

445 5.2. Shape sensing

446 When the ability of optical multicore fiber and multi-fiber sensors to sense curvature was widely
447 recognized, research efforts focused on shape reconstruction, obtained through curvature
448 integration. In 2004, Miller et al. proposed an approach to reconstruct the two-dimensional shape
449 of an optical multicore fiber with embedded FBGs based on the local curvature estimated from
450 distributed strain measurements [146]. The shape reconstruction algorithm estimated the local shape
451 utilizing osculating (or tangential) circles of curvature equal to the curvature measured. Finally, the
452 fiber shape was reconstructed as a sequence of arc segments separated by the grating spacing.
453 Zhanget al. (2004) developed a sensor device comprising a plurality of FBG sensors mounted on
454 the body of a flexible wire and able to sense shape in real-time [147]. The curvature was calculated
455 from the strain measured in the FBGs and interpolated between the sensor nodes. The shape was
456 then reconstructed as a sequence of arc segments with varying curvature.

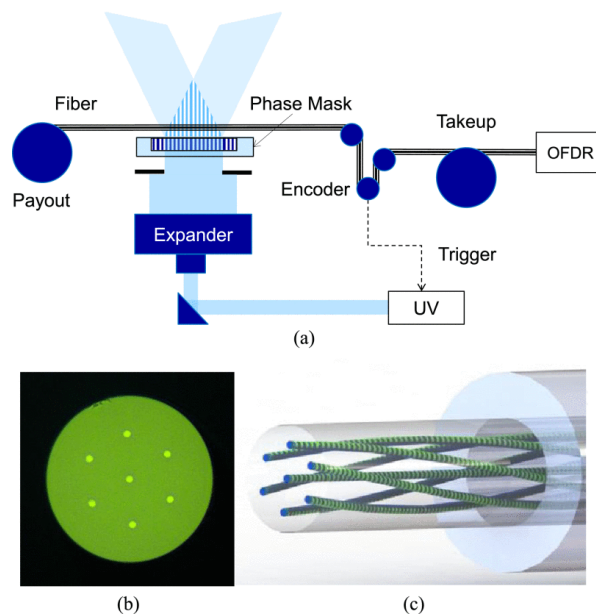
457 With the consolidation of approaches for distributed strain sensing, the first studies on distributed
458 shape sensing were carried out. In 2007, Duncan et al. measured shape and position of an optical
459 multicore fiber under a variety of circumstances using two sensing techniques: fiber Bragg gratings
460 and Rayleigh backscatter, and drew a comparison between the results of the measurements [149].
461 In 2008, Froggatt and Duncan filed a patent describing a fiber optic position and/or shape sensor
462 based on Rayleigh scatter and optical multicore fiber [150].

463 Previously, research and development efforts mainly centered on two-dimensional shape sensing,
464 while the performance of three-dimensional shape sensors was unsatisfactory and the shape
465 reconstruction algorithms notably complex. A significant improvement was then brought in by
466 Moore and Rogge, who developed, in 2012, an innovative approach for three-dimensional shape
467 reconstruction, based on the numerical resolution of a set of Frenet-Serret equations [93,151]. The
468 method offered remarkable advantages over previous approaches, determining complex three-
469 dimensional shapes as a continuous parametric solution rather than an integrated series of discrete
470 planar bends. Employing the aforementioned approach, Zhao et al. (2016) first utilized Brillouin
471 scattering to perform distributed shape sensing based on a 7-core multicore fiber [109].

472 Thanks to the technological developments and their remarkable advantages, fiber optic shape
473 sensing has found applications in several fields and a number of instruments based on this
474 technology have been developed [68,90,95,98,100,147,157–161]. By way of example, Chan and
475 Parker filed a patent in 2015 describing a method for rendering the shape of an optical multicore
476 fiber or multi-fiber bundle in three-dimensional space and in real time based on measured fiber
477 strain data with a range of applications, such as manufacturing, construction, medicine and
478 aerospace.[162]. Khan et al. developed (2019) a shape sensor based on optical multicore fiber with
479 fiber Bragg gratings to sense the shape of flexible medical instruments, such as catheters and
480 endoscopes (see Fig. 8) [158].

481 5.3. Twisting sensing

482 Due to the high flexibility, in addition to bending and longitudinal strain, FOSSs are oftentimes
 483 subject to twisting that generates significant errors in shape sensing [86,152,163–165]. The effects
 484 of the external twisting were first studied by Askins et al., who proposed, in 2008, a method for
 485 estimating the twisting of an optical fiber from internal strain state and designed a large-scale model
 486 of a tether fiber, 100X, to study this phenomenon [105]. Performing twisting measurements with
 487 FOSSs is extremely challenging, since the state of strain generated by twisting is quite modest, due
 488 to the small core spacing [86,152]. A solution to overcome the effects of twisting was designed by
 489 Westbrook et al. of OFS Labs. (2014), who manufactured an optical twisted seven-core multicore
 490 fiber for sensing applications (inscription apparatus and fiber are illustrated in Fig. 9) with fiber
 491 Bragg gratings inscribed along its length and with a twist of 50 turns per meter to increase the
 492 twisting sensitivity [91,92]. The optical multicore fiber could be interrogated using two different
 493 types of sensing signals: the FBGs inscribed into the optical fiber cores (enhanced signal) or the
 494 light scattering from the inherent Rayleigh scattering of the fiber cores. In this way, the fiber
 495 twisting could be calculated as the difference between the state of strain of outer and central cores,
 496 even if no experiment was performed to investigate the accuracy in twisting sensing. One year later,
 497 Cooper et al. of Fibercore designed and fabricated an optical spun (or twisted) multicore fiber for
 498 communications and sensing applications with a spin pitch of 15.4 mm (64.9 turn/m) [108,112].
 499
 500



501

502 **Fig. 9.** (a) Array inscription apparatus for continuous fabrication of gratings in all cores through UV
 503 transparent coating. (b) Cross-section of an optical seven-core fiber with coating removed. (c) Twisted
 504 multicore fiber schematic [33,92].

505 To the authors’ best knowledge, the research works by Xu et al. [153] and Galloway et al. [90]
 506 describe the first implementations of twisted FOSSs in sensing applications, specifically to track
 507 the complex motion of a continuum of robots and soft actuators.
 508 The accuracy of fiber optic shape sensors based on MCF in sensing twisting was investigated in
 509 [86,152] and will be discussed more profoundly in Section 7.

510 6. Applications

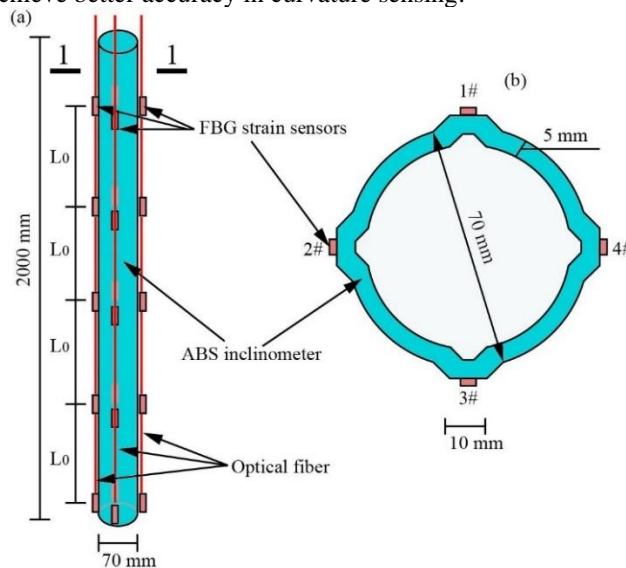
511 When optical fiber shape sensing became a mature technology, the attention of scientists and
 512 engineers was directed to its possible applications in virtue of its notable advantages compared to
 513 existing shape sensing methods. This section reviews the current state of the art on applications
 514 where fiber optic shape sensing has significant potential, with particular emphasis on the research
 515 works, in which this technology was utilized.

516 6.1. Civil engineering

517 6.1.1. Geotechnical monitoring

518 Landslides and slope movements are a significant hazard that can result in many fatalities and much
 519 property loss [166,167]. Geotechnical monitoring consists of continuous measurements and real-
 520 time analysis of the main geotechnical and environmental parameters in order to detect anomalous
 521 behavior in the initial phases and promptly intervene. Geotechnical inclinometers are used to
 522 determine the shape of ground movements, including the following data: direction, magnitude, rate
 523 and depth [17]. Such information is of essential importance to understand the behavior of landslides
 524 and slope movements and to develop intervention strategies [168]. Thanks to their resistance to
 525 corrosion, the capability of sensing shape with no visual contact and performing continuous and
 526 real-time monitoring, optical fiber shape sensors are particularly fit for purpose.

527 For these reasons, a lot of research has been concentrated on the development of fiber optic
 528 inclinometers. Some authors have exploited the capabilities of MCFs to develop monolithic
 529 inclinometers [169,170]. In fact, the extremely advanced drawing process of optical multicore fibers
 530 guarantees compactness and high manufacturing accuracy, while the small core spacing ensures
 531 minimal temperature gradients. More extensive research has been focused on the design of
 532 distributed optical multi-fiber inclinometers for ground movement monitoring, obtained by
 533 fastening several optical fibers with embedded strain sensors to a tube or a bar, as shown in Fig. 10
 534 [96,97,99,171,172]. These sensors are essentially cantilever beams with one end fixed. The section
 535 geometries have the same configuration as optical multicore fibers (three-core or four-core
 536 configuration), but with greater core spacing, which differs by several orders of magnitude from
 537 MCFs in order to achieve better accuracy in curvature sensing.



538

539

Fig. 10. (a) Schematic diagram of FBG-based inclinometer; (b) Cross-section [99].

540 6.1.2. Structural health monitoring of civil infrastructures

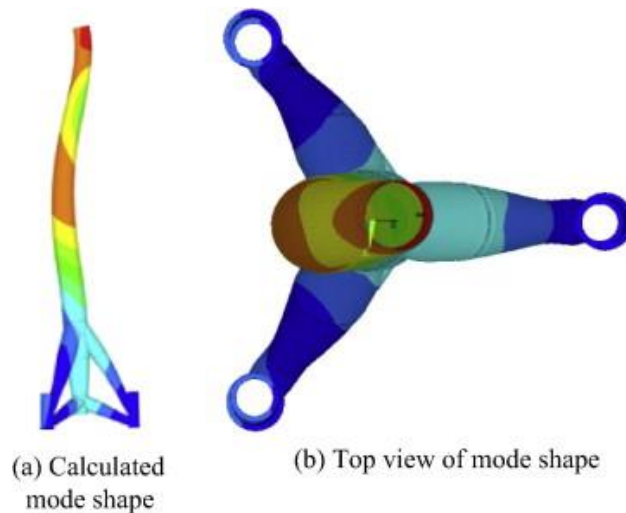
541 Structural health monitoring systems provide information about the performance and conditions of
542 structures and infrastructures through the observation of their in-service behaviors [27]. For this
543 purpose, fiber optic shape sensing can represent an efficient nondestructive method for the direct,
544 continuous and real-time monitoring of deformed structural shape and the interpretation of the
545 global structural behavior.

546 MacPherson et al. first proposed an application in tunnel health monitoring of multiplexed fiber
547 Bragg grating strain sensors based on multicore fiber [173]. A sensor, consisting of a series of
548 gratings, inscribed in the cores of an optical four-core fiber, and able to measure curvature along its
549 length, was configured to monitor displacement between the segments of a concrete tunnel section
550 and was able to reach a resolution of ± 0.1 mm.

551 To the best knowledge of the authors, fiber optic shape sensing has not been employed in bridge
552 health monitoring. Nevertheless, its capabilities of direct shape sensing and continuous evaluation
553 of the structural efficiency during the phases of construction and under service loads have great
554 potential in this field [174–179]. By way of example, Kissinger et al. designed a dynamic fiber optic
555 shape sensor based on multiplexed Bragg gratings inscribed in 4 fibers attached to a flexible support
556 that can be employed to study the response of bridges under dynamic loads [180]. The sensor was
557 tested using a cantilever test object and was able to measure structural displacements and vibrations
558 over an interferometric bandwidth of 21 kHz. In addition, it has been demonstrated that the
559 deflection of a bridge span under designed loads, an important parameter for bridge safety
560 evaluation, can be efficiently measured by using inclinometers similar to those described above for
561 geotechnical inclinometers [18].

562 Another potential application of fiber optic shape sensors is the monitoring of verticality and
563 deformation of buildings, bridge piles and towers [101,181]. Bang et al. developed a sensor
564 composed of an array of multiplexed FBGs for the measurement of strain and bending deflection
565 of an 1.5 MW wind turbine tower [182]. With the aim of monitoring the dynamic structural behavior
566 of the wind turbine, 10 FBG sensors were arranged on the inner surface of the tower facing the
567 prevailing wind. Similar analyses could be performed by using fiber optic shape sensors with the
568 significant advantage of determining the three-dimensional deformed shape of wind towers (an
569 example is shown in Fig. 11) with a single and easily installable cable.

570



571

572

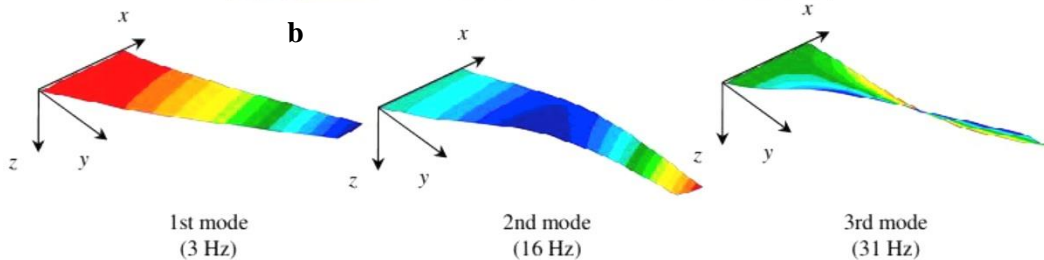
Fig. 11. Calculated mode shape of the wind turbine tower [183].

573 Thanks to their resistance to high-energy ionizing environments, as demonstrated in [184], FOSSs
 574 are particularly suitable for the structural health monitoring of nuclear power stations and spent
 575 nuclear fuel stores, which is of vital importance considering that radiation can be extremely
 576 hazardous to humans or to the environment.

577 6.2. Industrial and aerospace engineering

578 6.2.1. Aircraft Wing Shape Measurement

579 The reconstruction of the displacement field is a fundamental capability for structural health
 580 monitoring critical components. One of the common problems in aerospace engineering is the
 581 determination of the shape of wings through strain measurements (Fig. 12). The most widely used
 582 approaches to achieve this goal are: the inverse Finite Element Method, the Modal Method and Ko's
 583 Displacement Theory, comprehensively reviewed in [185]. The three methods require a heavy
 584 computational cost in addition to the use of a considerable number of strain sensors.
 585



588 **Fig. 12.** Aircraft wing shape sensing by using strain sensors: (a) aluminum wing-shaped plate deflected
 589 under its own weight; (b) first three mode shapes and corresponding natural frequencies [185].

590 Optical fiber strain sensors have revolutionized the sector and brought remarkable improvements,
 591 thanks to their advantages over traditional electrical sensors, such as anti-electromagnetic
 592 interference, resistance to corrosion and harsh environments, multiplexing ability and the capability
 593 of adapting to complex environments [120,186,187]. Nonetheless, fiber optic shape sensing can
 594 bring even more significant enhancements, offering an alternative to traditional methods for
 595 dynamic and direct shape measurements with no need for developing computational models. In
 596 2006, Klute et al. of Luna Innovations developed a new shape sensing technology which enables
 597 the distributed and axially co-located differential strain measurements based on optical multicore
 598 fiber and OFDR. This approach generates complex shape data of Variable Geometry Chevron
 599 (VGC) that is a (NiTiInol) actuator-based morphing system, flight tested by Boeing shortly before
 600 [163].

601 6.3. Medical applications

602 6.3.1. Robotics

603 FOSSs have a great potential for the implementation in two emerging classes of robots: continuum
604 robots and soft robots.

605 Continuum robots are “invertebrate-like” or “snake-like” robotic systems, consisting of
606 continuously curving manipulators, highly suitable for surgical interventions, thanks to their high
607 dexterity, in addition to flexibility and small size. The implementation of shape sensors, providing
608 a dynamic feedback on shape and position of these instruments, allows for more accurate control
609 and enables minimally invasive and precise surgery. Xu et al. designed an innovative helically
610 wrapped FBG sensor and a novel theoretical approach to measure simultaneously curvature, torsion,
611 and force [153]. Two sensorized Nitinol tubes were manufactured and tested to validate the design
612 and the model and their ability to accurately measure curvature, torsion, and force at a 100 Hz
613 sampling rate was confirmed.

614 Soft robots are robotic system composed of flexible and easily deformable materials (as illustrated
615 in the figure below), such as elastomers, gels, fluids, and able to perform complex deformations
616 with simple inputs, mimicking the compliance and mechanical properties of biological organisms
617 [188,189]. Soft robots, in virtue of their extraordinary adaptability and flexibility, are particularly
618 apt for applications fields of medicine and biomedicine [190], and offer a valid alternative to
619 traditional rigid-robotic systems that commonly have limited configurations determined by the joint
620 motions.



621

622

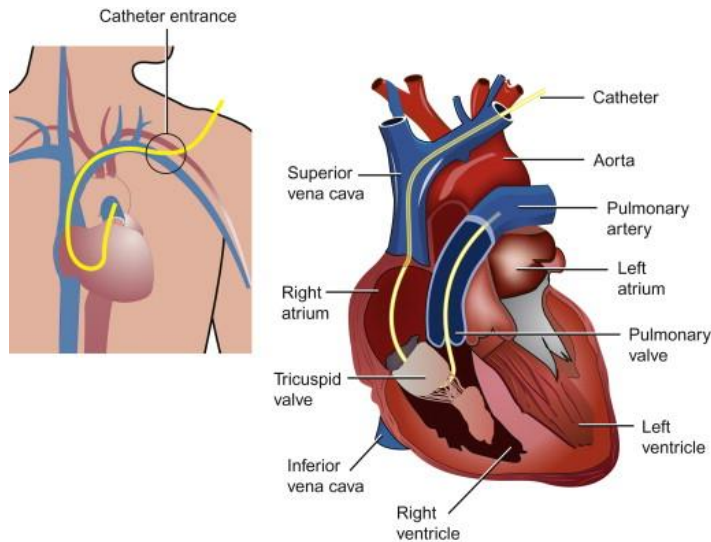
Fig. 13. Examples of soft robots [189].

623 Unfortunately, one of the critical disadvantages of soft robotics is the lack of systems capable of
624 collecting high-resolution shape information [90,188,191,192]. The research conducted by Li et al.
625 [192] and Wang et al. [191] have proved that the employment of FBG sensors can be an efficient
626 solution for shape tracking soft manipulators. Fiber optic shape sensors, by virtue of their
627 embedding capability, compactness and high flexibility, are highly suitable for this purpose.
628 Galloway et al. first implemented a monolithic FOSS in the structure of a fiber-reinforced soft
629 actuator. The optical twisted 4-core MCF sensor interrogated by way of optical frequency domain
630 reflectometry was able to sense shape, position and body twisting with submillimetric resolution
631 [90].

632 6.3.2. Surgical instruments

633 During surgical interventions the dynamic tracking of shape and position of medical instruments
634 inside the human body is crucial to ensure accurate manipulation and minimal invasivity [193]. As
635 previously discussed in Section 2.6, fluoroscopy, one of the most frequently used approaches for
636 this purpose during clinical procedures [57–61], has several disadvantages, including high cost,

637 bulkiness, low-speed data acquisition and, foremost, exposure to radiation [57,58]. A widespread
 638 alternative practice is the determination of the position of catheters and needles inside the human
 639 body by their resistance, which evidently is an arbitrary evaluation criterion.
 640 Fiber optic shape sensors have great potential in numerous medical applications, including epidural
 641 administration [68], colonoscopy [157,158], ophthalmic and cardiac procedures (illustrated in Fig.
 642 14) [160], endovascular navigation [159], biopsy [158,160] and minimally invasive surgery
 643 [100,161], since they can be efficiently implemented in different medical equipment, such as
 644 catheters, needles, and endoscopes, owing to their advantages: intrinsic safety, biocompatibility,
 645 embedding capability, flexibility, compactness, light weight and small size. The following are some
 646 examples of FOSS integration in surgical instruments.
 647



648

649

Fig. 14. Thermistor catheter for temperature measurement in the pulmonary artery [194].

650 A fiber optic shape sensor for intelligent colonoscopy was proposed by Zhang et al. in 2014 [147].
 651 The sensor, consisting in a 900-mm-long flexible wire on which optical fibers were mounted with
 652 inscribed FBGs, was implemented in a colonoscope and tested in the colon of a live pig, and was
 653 able to reconstruct the shape of the instrument. In 2014, Moon et al. designed a thin and highly
 654 flexible FOSS, integrable into minimally invasive surgical systems and capable of dynamic and
 655 real-time shape tracking (sampling rate of 3.74 Hz) with an average position error at the extremity
 656 of 1.50% of the total sensing length [100]. The sensor was manufactured by assembling and epoxy
 657 gluing 3 optical fibers with embedded fiber Bragg gratings in triangular configuration and had a
 658 length of 115 mm and could bend up to 90°. Roesthuis et al. (2014) developed a prototype of a
 659 flexible nitinol (NiTi) needle with an integrated array of 12 FBGs sensors to enable 3D real-time
 660 needle steering [98]. The sensor was able to sense axial strain, curvature and shape with maximum
 661 errors between the experiments and the results determined from a model based on the beam theory
 662 equal to 0.20, 0.51 mm and 1.66 mm, taking into account the in-plane deflection with single
 663 bending, in-plane deflection with double bending and out-of-plane deflection. In 2019, Jäckle et al.
 664 designed a MCF-based shape sensor for endovascular navigation [159] by inscribing a set of FBGs
 665 written into the 3 cores of a 7-core multicore fiber and was able to measure curvature and track
 666 shape. An advanced approach for shape reconstruction was formulated to enhance sensor accuracy
 667 that sensed shape with an average error of 0.35–1.15 mm and maximal error of 0.75–7.53 mm over
 668 the entire sensor length of 380mm. Khan et al. presented (2019) an innovative method for the shape

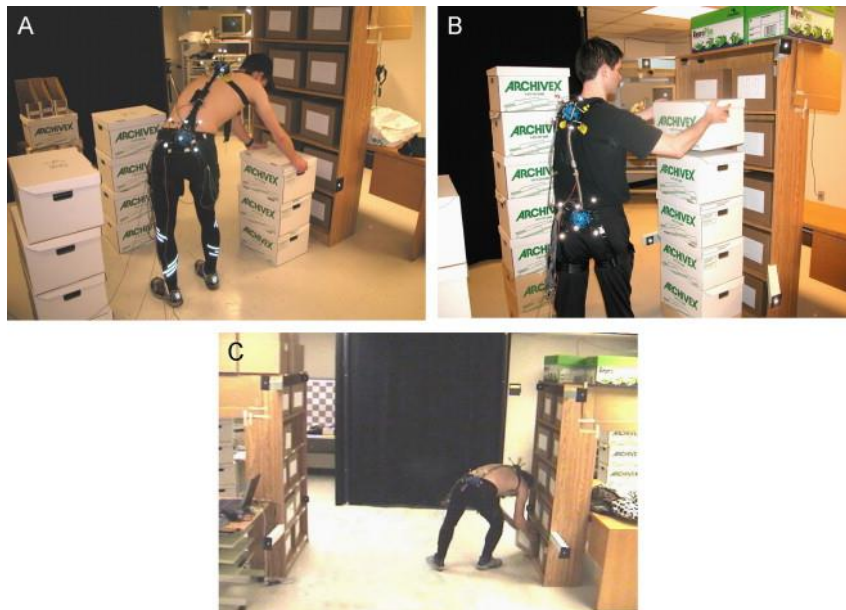
669 reconstruction of flexible medical instruments in three-dimensional Euclidean space using multiple
670 MCFs with inscribed FBGs [158]. This method was used to develop a novel sensing system,
671 consisting of a multi-segment catheter sensorized by inserting four multicore fibers. Experimental
672 tests in diverse configurations demonstrated its ability to sense shape with high accuracy (maximum
673 absolute error of 1.05 mm and maximum mean error of 0.44 mm).

674 The ability of medical instruments to detect force has been demonstrated to support the correct
675 identification of their location inside the human body with limited tissue damage [68]. In 2017,
676 Khan et al. developed a force and shape fiber optic sensor able to simultaneously estimate the shape
677 of medical instruments and the interaction forces with the surrounding environment [95]. The sensor
678 was composed of 3 optical single-core fibers with inscribed FBGs in a triangular configuration
679 (constant angular space of 120°).

680 6.3.3. Posture monitoring

681 Another possible application of fiber optic shape sensing in the medical field is the detection of
682 spinal posture changes. In 2006, Plamondon et al. conducted an experimental study to evaluate a
683 hybrid system composed of two inertial sensors for the three-dimensional measurement of trunk
684 posture, as shown in Fig. 15 [13]. A year later, Wong and Wong proposed a method for monitoring
685 sitting postural changes using 3 tri-axial accelerometers [7]. Artem et al. (2015) developed a tape
686 sensor composed of interconnected and programmable sensor nodes on a flexible electronics
687 substrate and proposed it be used as a wearable posture monitoring device with a deformation
688 sensing algorithm [14]. Compared with these existing methods, shape sensing based on optical fiber
689 has several advantages, particularly suitable for this application scenario: compactness, flexibility,
690 light weight, high sensitivity and accuracy, high frequency data acquisition and embedding and
691 multiplexing capability.

692



693

694 **Fig. 15.** Experimental setup of the hybrid system for three-dimensional trunk posture measurement: (a) static
695 validation; (b) short dynamic validation; (c) long dynamic validation [13].

696 7. Error analysis

697 Several experimental studies have investigated the accuracy of fiber optic shape sensors. It was
698 found that the average accuracy of these sensors in position and shape measurements is ~ 1 mm
699 [98,149,158,159,161,165,195,196], nevertheless, in some cases, FOSSs achieve submillimetric
700 accuracy [83,90,197]. Regrettably, it is not possible to draw a comparison among the vast multitude
701 of optical-fiber-based shape sensors reported in the literature since their accuracy was not assessed
702 in standardized conditions. Sensor length and the complexity of the shape measured varied widely,
703 parameters that greatly influence their accuracy. Research studies on the error sources of these
704 sensors are extremely limited. The most important are examined below.

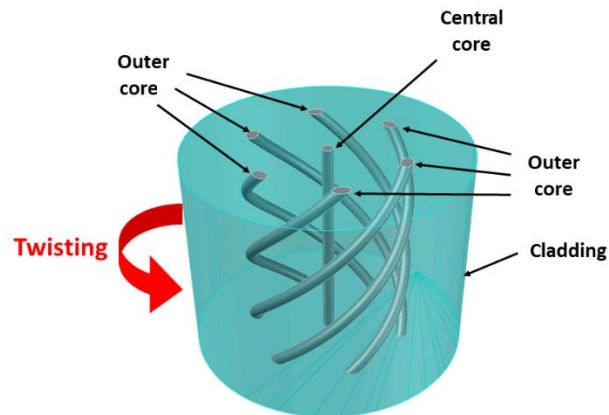
705 High-accuracy shape sensing cannot be separated from efficient strain sensing. In this respect, an
706 experimental study was conducted by Floris et al. in order to define how strain sensor length affects
707 the shape reconstruction performance of FBG-based FOSSs, the most widely used typology of fiber
708 optic shape sensors [83,198]. Two FOSSs were manufactured by the inscription of long and short
709 FBGs, 8.0 mm and 1.5 mm long, into the cores of a commercial MCF. The shape sensor
710 performance was assessed by sensing the shape of a sequence of semi-circles on an aluminum mold
711 by means of a high-precision Computer Numerical Controlled (CNC) machine. Finally, it was
712 proved that shape sensors based on long-FBGs are remarkably more efficient in sensing strain,
713 curvature and shape, in virtue of the stronger and more easily detectable wavelength peak, and better
714 able to average the local errors because of the longer length.

715 Ordinarily, strain sensors are uniformly distributed along the length of a shape sensor, with a
716 constant center-to-center distance. This is valid for both FBG-based shape sensors and distributed
717 shape sensors; in this last case, the center-to-center distance is equal to the spatial resolution. In
718 each instrumented section, the curvature is determined from the values of strain. Thus, in the non-
719 instrumented portions of the shape sensor, the missing curvatures are determined by interpolation.
720 Finally, the shape of the sensor is reconstructed through numerical integration of the curvature.
721 Hence, it is evident that curvature interpolation is a source of errors in shape sensing, which
722 becomes more relevant with the increase of the distance between the strain sensors. Jäckle et al.
723 investigated the influence of the curvature interpolation method on shape reconstruction, estimating
724 by means of simulations the accuracy of an FBG-based FOSS in sensing the shape of an arc and an
725 s-curve. Three interpolation methods were analyzed: nearest neighbor, cubic and averaged cubic;
726 and the last one was demonstrated to be the most efficient at equal number of measurement points
727 [199].

728 As mentioned in Section 5.3, external twisting is a significant source of errors in fiber optic shape
729 sensing [163–165], although most of the approaches for shape sensing neglect this phenomenon
730 [93,95,147,180,197]. The first study on this subject was conducted by Askins et al., who presented
731 a method for determining the twisting of optical fibers and manufactured a large-scale model (100X)
732 of a tether fiber to assess the correctness of the method [105], since the twisting sensitivity increases
733 with increased core spacing [86]. Regrettably, the increase of core spacing reduces the flexibility
734 and embedding capability of shape sensors, restricting their field of applications. Thanks to
735 important improvements in the manufacturing process [91,92,108,112] it has become possible to
736 make twisted MCFs to enhance accuracy in twisting sensing without compromising sensor
737 flexibility.

738 Floris et al. first assessed the performance of a twisted MCF-based shape sensor in sensing twisting
739 [86,152]. A theoretical approach, based on Saint-Venant's Torsion Theory, was proposed to
740 determine the twisting in the MCF from the strain sensed in the cores, as illustrated in Fig. 16. On
741 the basis of this approach, the mathematical relationship between twisting sensitivity and core
742 spacing and twisting rotation were defined. A twisted FOSS was produced by inscribing four FBGs
743 in a commercial spun MCF with a spin pitch of 15.4 mm manufactured by Fibercore [108,112], and
744 the validity of the theoretical approach was experimentally demonstrated with a series of twisting
745 tests. An enhanced method of shape reconstruction was proposed to take into account and

746 compensating the twisting.



747

748

Fig. 16. Twisted multicore seven-core fiber [86].

749 In conclusion, several numerical studies were undertaken to simultaneously investigate and evaluate
750 the influence of different variables on the accuracy of fiber optic shape sensors.

751 Henken et al. performed an error analysis to quantify the accuracy of FBG-based shape sensors with
752 a three-core configuration and to assess their suitability for robotic medical needle steering [164].
753 Several parameters that influence shape reconstruction accuracy were considered in the simulations,
754 including: measured wavelength inaccuracy, photoelastic coefficient, sensor geometry inaccuracies
755 (errors in core spacing and angular spacing), and the measured curvature inaccuracies. It was found
756 that the accuracy of FBG-based shape sensors implemented in needles can be in the order of 10%
757 of the deflection at the tip, depending on the configuration. Nevertheless, when tip deflection is
758 smaller than approximately 1 mm it cannot be detected accurately.

759 Floris et al. conducted two numerical studies to analyze the effects of core position errors and strain
760 measurement uncertainty on the performance of fiber optic shape sensors used to sense three-
761 dimensional curvature, which is a fundamental step in the process of shape reconstruction
762 [84,85,200]. The studies, applicable to shape sensors based on both MCF and multiple single-core
763 fibers equipped with distributed or quasi-distributed strain-sensors, determined the law of
764 uncertainty propagation by simulating the measurement process through the Monte Carlo Method
765 (MCM) and showed the crucial role played by different parameters, including core spacing,
766 curvature measured and number of cores. Ultimately, a series of predictive models were proposed,
767 described by simple equations and capable of predicting the achievable FOSS performance in
768 diverse conditions.

769 **8. Conclusions and future research**

770 An enormous research effort has been devoted to the development of a new generation of shape
771 sensors based on optical fiber sensing technology. The reasons behind the interest in this innovative
772 technology are its ground-breaking advantages that make it extremely competitive against existing
773 shape tracking methods. This paper has presented a comprehensive review of the state-of-the-art of
774 fiber optic shape sensing from its historical evolution to its application.

775 This review will help scientists and industries in the field to have a panoramic and concise overview
776 of the subject, raise awareness to the potential and criticalities of this novel technology and provide
777 inspiration for future investigations. On the basis of this review, the following observations and
778 conclusions can be drawn:

- 779
- 780
- 781
- 782
- 783
- 784
- 785
- 786
- 787
- 788
- 789
- 790
- 791
- 792
- 793
- 794
- 795
- 796
- 797
- 798
- 799
- 800
- 801
- 802
- 803
- 804
- 805
- 806
- 807
- 808
- 809
- 810
- 811
- 812
- 813
- 814
- 815
- FOSSs provide a valid alternative to traditional shape sensing methods, thanks to a combination of exceptional advantages, including capability of tracking shape directly, continuously, dynamically and in real-time, no necessity for visual contact, embedding capability, ease of installation, compactness, small size, flexibility, immunity to electromagnetic interference, intrinsic safety, resistance to corrosion and harsh environments;
 - FOSSs can be primarily divided into two main categories: MCF-based and multi-fiber-based. The first category is characterized by monolithicity, compactness, small size, high-precision manufacturing and ease of assembly. Such characteristics make it particularly suitable for the implementation in medical instruments, such as needles, catheters and endoscopes and in small instruments in general. The second, instead, in virtue of its larger core spacing, achieves higher accuracy in shape reconstruction in equal conditions and finds applications in the medical tracking devices as well as in geotechnical and structural health monitoring, for instance to reconstruct the deformed shape of structures and components – characterized by limited deformability –, common in civil, aerospace and mechanical engineering;
 - Another possible FOSS category is based on the technology used to sense strain; the most commonly employed are: quasi-distributed (fiber Bragg grating) and distributed (Rayleigh and Brillouin backscattering). FBG-based FOSSs are the most widely used thanks to the vastly lower cost of their interrogation systems and to higher speed data acquisition (~ kHz), which make this technology suitable for dynamic sensing. Distributed strain sensing systems can enhance sensing length and achieve higher accuracy in shape sensing. This last case occurs when the spatial resolution is particularly high (spatial resolution lower than center-to-center distance of the gratings in FBG-based shape sensors);
 - The average accuracy of FOSSs in position and shape measurements is ~1 mm [98,149,158,159,161,165,195,196], although, in some cases, submillimetric accuracy was demonstrated [83,90,197]. Unfortunately, a comparison of the performance among the large number of FOSSs reported until now is not possible, since their accuracy was assessed in non-standardized conditions and with widely varying length and complexity of the shape measured, parameters that greatly influence sensor performance.
 - In spite of the large amount of research dedicated to the development of fiber optic shape sensing and its great potential, the overwhelming majority of studies on its applications belong to the medical or geotechnical fields. An in-depth study on the employment of FOSSs in a number of other possible applications (see Section 6) including structural health monitoring of buildings, bridges, tunnels and mechanical components, and the tracking of human posture and robot movements, is still missing. Future research directed to bridging this gap would substantially contribute to the diffusion of this technology.

816 Acknowledgments

817 This work was carried out within the ITN-FINESSE framework, funded by the European Union's
818 Horizon 2020 Research and Innovation Program under the Marie Skłodowska-Curie Action Grant
819 Agreement N° 722509. It was also supported by the Ministry of Economy and Competitiveness of
820 Spain under DIMENSION TEC2017-88029-R.

821

References

- 822 [1] Koch E, Dietzel A. Surface reconstruction by means of a flexible sensor array. *Sensors Actuators A Phys*
823 2017;267:293–300. doi:10.1016/j.sna.2017.10.023.
- 824 [2] Wang Q, Liu Y. Review of optical fiber bending/curvature sensor. *Meas J Int Meas Confed* 2018;130:161–76.
825 doi:10.1016/j.measurement.2018.07.068.

- 826 [3] Schaefer P-L, Barrier G, Chagnon G, Alonso T, Moreau-Gaudry A. Strain Gauges Based 3D Shape Monitoring of
827 Beam Structures Using Finite Width Gauge Model. *Exp Tech* 2019;43:599–611. doi:10.1007/s40799-019-00312-
828 4.
- 829 [4] Porcu MC, Patteri DM, Melis S, Aymerich F. Effectiveness of the FRF curvature technique for structural health
830 monitoring. *Constr Build Mater* 2019;226:173–87. doi:10.1016/j.conbuildmat.2019.07.123.
- 831 [5] Frau A, Pieczonka L, Porcu MC, Staszewski WJ, Aymerich F. Analysis of elastic nonlinearity for impact damage
832 detection in composite laminates. *J Phys Conf Ser* 2015;628:012103. doi:10.1088/1742-6596/628/1/012103.
- 833 [6] Porcu MC, Pieczonka L, Frau A, Staszewski WJ, Aymerich F. Assessing the Scaling Subtraction Method for
834 Impact Damage Detection in Composite Plates. *J Nondestruct Eval* 2017;36:33. doi:10.1007/s10921-017-0413-9.
- 835 [7] Wong WY, Wong MS. Detecting spinal posture change in sitting positions with tri-axial accelerometers. *Gait
836 Posture* 2008;27:168–71. doi:10.1016/j.gaitpost.2007.03.001.
- 837 [8] Hermanis A, Cacurs R, Greitans M. Acceleration and Magnetic Sensor Network for Shape Sensing. *IEEE Sens J*
838 2016;16:1271–80. doi:10.1109/JSEN.2015.2496283.
- 839 [9] Stollenwerk K, Müllers J, Müller J, Hinkenjann A, Krüger B. Evaluating an Accelerometer-Based System for
840 Spine Shape Monitoring. In: Gervasi O, Murgante B, Misra S, Stankova E, Torre CM, Rocha AMAC, et al.,
841 editors. *Int. Conf. Comput. Sci. Its Appl.*, vol. 10963, Cham: Springer International Publishing; 2018, p. 740–56.
842 doi:10.1007/978-3-319-95171-3_58.
- 843 [10] Hermanis A, Nesenbergs K. Grid shaped accelerometer network for surface shape recognition. 2012 13th Bienn.
844 Balt. Electron. Conf., IEEE; 2012, p. 203–6. doi:10.1109/BEC.2012.6376852.
- 845 [11] de Gelidi S, Seifnaraghi N, Bardill A, Tizzard A, Wu Y, Sorantin E, et al. Torso shape detection to improve lung
846 monitoring. *Physiol Meas* 2018;39:074001. doi:10.1088/1361-6579/aacc1c.
- 847 [12] Washizawa S, Nakata Y, Uchida D, Maeda K, Inomata A, Yaginuma Y. Estimation of spinal shape profiles in
848 motion using accelerometers. *IEEE SENSORS 2014 Proc.*, vol. 2014- Decem, IEEE; 2014, p. 2238–41.
849 doi:10.1109/ICSENS.2014.6985486.
- 850 [13] Plamondon A, Delisle A, Larue C, Brouillette D, McFadden D, Desjardins P, et al. Evaluation of a hybrid system
851 for three-dimensional measurement of trunk posture in motion. *Appl Ergon* 2007;38:697–712.
852 doi:10.1016/j.apergo.2006.12.006.
- 853 [14] Dementyev A, Kao HLC, Paradiso JA. SensorTape: Modular and programmable 3D-aware dense sensor network
854 on a tape. *UIST 2015 - Proc 28th Annu ACM Symp User Interface Softw Technol* 2015:649–58.
855 doi:10.1145/2807442.2807507.
- 856 [15] Griffith C, Dare P, Danish L. Calibration enhancement of ShapeAccelArray technology for long term deformation
857 monitoring applications. *IEEE/ION Position, Locat. Navig. Symp.*, IEEE; 2010, p. 621–6.
858 doi:10.1109/PLANS.2010.5507183.
- 859 [16] Green E, Mikkelsen PE. Deformation Measurements with Inclinometers 1952.
- 860 [17] Stark TD, Choi H. Slope inclinometers for landslides. *Landslides* 2008;5:339–50. doi:10.1007/s10346-008-0126-
861 3.
- 862 [18] Hou X, Yang X, Huang Q. Using Inclinometers to Measure Bridge Deflection. *J Bridg Eng* 2005;10:564–9.
863 doi:10.1061/(ASCE)1084-0702(2005)10:5(564).
- 864 [19] Cha Y-J, Choi W, Büyükköztürk O. Deep Learning-Based Crack Damage Detection Using Convolutional Neural
865 Networks. *Comput Civ Infrastruct Eng* 2017;32:361–78. doi:10.1111/mice.12263.
- 866 [20] Ye XW, Dong CZ, Liu T. A Review of Machine Vision-Based Structural Health Monitoring: Methodologies and
867 Applications. *J Sensors* 2016;2016:1–10. doi:10.1155/2016/7103039.
- 868 [21] Milillo P, Porcu MC, Lundgren P, Soccodato F, Salzer J, Fielding E, et al. The ongoing destabilization of the
869 mosul dam as observed by synthetic aperture radar interferometry. 2017 IEEE Int. Geosci. Remote Sens. Symp.,
870 vol. 7, IEEE; 2017, p. 6279–82. doi:10.1109/IGARSS.2017.8128442.
- 871 [22] Gentile C. Application of Radar Technology to Deflection Measurement and Dynamic Testing of Bridges. *Radar
872 Technol.*, vol. 395, InTech; 2010, p. 116–24. doi:10.5772/7178.
- 873 [23] Gentile C, Bernardini G. Radar-based measurement of deflections on bridges and large structures. *Eur J Environ
874 Civ Eng* 2010;14:495–516. doi:10.1080/19648189.2010.9693238.
- 875 [24] Choi S, Kim B, Lee H, Kim Y, Park H. A Deformed Shape Monitoring Model for Building Structures Based on a
876 2D Laser Scanner. *Sensors* 2013;13:6746–58. doi:10.3390/s130506746.
- 877 [25] Mentzer MA. *Fiber Optic Sensors*. vol. 20020456. CRC Press; 2002. doi:10.1201/9780824744571.
- 878 [26] Campanella C, Cuccovillo A, Campanella C, Yurt A, Passaro V. Fibre Bragg Grating Based Strain Sensors:
879 Review of Technology and Applications. *Sensors* 2018;18:3115. doi:10.3390/s18093115.
- 880 [27] López-Higuera JM, Cobo LR, Incera AQ, Cobo A. Fiber optic sensors in structural health monitoring. *J Light
881 Technol* 2011;29:587–608. doi:10.1109/JLT.2011.2106479.
- 882 [28] Lee B. Review of the present status of optical fiber sensors. *Opt Fiber Technol* 2003;9:57–79. doi:10.1016/S1068-
883 5200(02)00527-8.
- 884 [29] Rao Y-J. In-fibre Bragg grating sensors. *Meas Sci Technol* 1997;8:355–75. doi:10.1088/0957-0233/8/4/002.
- 885 [30] Correia R, James S, Lee S-W, Morgan SP, Korposh S. Biomedical application of optical fibre sensors. *J Opt
886 2018;20:073003*. doi:10.1088/2040-8986/aac68d.
- 887 [31] Barrias A, Casas J, Villalba S. A Review of Distributed Optical Fiber Sensors for Civil Engineering Applications.
888 *Sensors* 2016;16:748. doi:10.3390/s16050748.
- 889 [32] Leung CKY, Wan KT, Inaudi D, Bao X, Habel W, Zhou Z, et al. Review: optical fiber sensors for civil engineering

- 890 applications. *Mater Struct* 2015;48:871–906. doi:10.1617/s11527-013-0201-7.
- 891 [33] Amanzadeh M, Aminossadati SM, Kizil MS, Rakić AD. Recent developments in fibre optic shape sensing. *Meas*
892 *J Int Meas Conf* 2018;128:119–37. doi:10.1016/j.measurement.2018.06.034.
- 893 [34] Baqersad J, Poozesh P, Niezrecki C, Avitabile P. Photogrammetry and optical methods in structural dynamics –
894 A review. *Mech Syst Signal Process* 2017;86:17–34. doi:10.1016/j.ymsp.2016.02.011.
- 895 [35] Sun H, Xu Z, Yao L, Zhong R, Du L, Wu H. Tunnel Monitoring and Measuring System Using Mobile Laser
896 Scanning: Design and Deployment. *Remote Sens* 2020;12:730. doi:10.3390/rs12040730.
- 897 [36] Liu J, Zhang Q, Wu J, Zhao Y. Dimensional accuracy and structural performance assessment of spatial structure
898 components using 3D laser scanning. *Autom Constr* 2018;96:324–36. doi:10.1016/j.autcon.2018.09.026.
- 899 [37] Zheng D, Cai Z, Floris I, Madrigal J, Pan W, Zou X, et al. Temperature-insensitive optical tilt sensor based on a
900 single eccentric-core fiber Bragg grating. *Opt Lett* n.d. doi:10.1364/OL.99.099999.
- 901 [38] Bøving KG. Strain gauge technology. *NDE Handb. Non-Destructive Exam. Methods Cond. Monit., Elsevier*;
902 1989, p. 295–301. doi:10.1016/B978-0-408-04392-2.50035-7.
- 903 [39] Ajovalasit A. Advances in Strain Gauge Measurement on Composite Materials. *Strain* 2011;47:313–25.
904 doi:10.1111/j.1475-1305.2009.00691.x.
- 905 [40] Ye XW, Su YH, Han JP. Structural health monitoring of civil infrastructure using optical fiber sensing technology:
906 A comprehensive review. *Sci World J* 2014;2014. doi:10.1155/2014/652329.
- 907 [41] Annamdas KKK, Annamdas VGM. Review on developments in fiber optical sensors and applications. In: Mendez
908 A, Du HH, Wang A, Udd E, Mihailov SJ, editors. *Fiber Opt. Sensors Appl. VII*, vol. 7677, 2010.
909 doi:10.1117/12.849799.
- 910 [42] Masoudi A, Newson TP. Contributed Review: Distributed optical fibre dynamic strain sensing. *Rev Sci Instrum*
911 2016;87:011501. doi:10.1063/1.4939482.
- 912 [43] Haksoo Choi, Sukwon Choi, Hojung Cha. Structural Health Monitoring system based on strain gauge enabled
913 wireless sensor nodes. 2008 5th Int. Conf. Networked Sens. Syst., IEEE; 2008, p. 211–4.
914 doi:10.1109/INSS.2008.4610888.
- 915 [44] Jafarkhani R, Masri SF. Finite Element Model Updating Using Evolutionary Strategy for Damage Detection.
916 *Comput Civ Infrastruct Eng* 2011;26:207–24. doi:10.1111/j.1467-8667.2010.00687.x.
- 917 [45] He J, Zhou Y, Guan X, Zhang W, Wang Y, Zhang W. An Integrated Health Monitoring Method for Structural
918 Fatigue Life Evaluation Using Limited Sensor Data. *Materials (Basel)* 2016;9:894. doi:10.3390/ma9110894.
- 919 [46] Chang PC, Flatau A, Liu SC. Review Paper: Health Monitoring of Civil Infrastructure. *Struct Heal Monit An Int*
920 *J* 2003;2:257–67. doi:10.1177/1475921703036169.
- 921 [47] Xia Y, Hao H, Brownjohn JMW, Xia P-Q. Damage identification of structures with uncertain frequency and mode
922 shape data. *Earthq Eng Struct Dyn* 2002;31:1053–66. doi:10.1002/eqe.137.
- 923 [48] Mottershead JE, Friswell MI. Model Updating In Structural Dynamics: A Survey. *J Sound Vib* 1993;167:347–75.
924 doi:10.1006/jsvi.1993.1340.
- 925 [49] He W-Y, Ren W-X, Zuo X-H. Mass-normalized mode shape identification method for bridge structures using
926 parking vehicle-induced frequency change. *Struct Control Heal Monit* 2018;25:e2174. doi:10.1002/stc.2174.
- 927 [50] Sohn H, Farrar CR, Hunter NF, Worden K. Structural Health Monitoring Using Statistical Pattern Recognition
928 Techniques. *J Dyn Syst Meas Control* 2001;123:706–11. doi:10.1115/1.1410933.
- 929 [51] Shu T, Gharaty S, Xie W, Joubair A, Bonev IA. Dynamic Path Tracking of Industrial Robots With High Accuracy
930 Using Photogrammetry Sensor. *IEEE/ASME Trans Mechatronics* 2018;23:1159–70.
931 doi:10.1109/TMECH.2018.2821600.
- 932 [52] Agdas D, Rice JA, Martinez JR, Lasa IR. Comparison of Visual Inspection and Structural-Health Monitoring As
933 Bridge Condition Assessment Methods. *J Perform Constr Facil* 2016;30:04015049. doi:10.1061/(ASCE)CF.1943-
934 5509.0000802.
- 935 [53] Machan G, G. BV. Use of Inclinometers for Geotechnical Instrumentation on Transportation Projects - State of
936 the Practice. Transportation Research Board Soils and Rock Instrumentation Committee Engineering Geology
937 Committee; 2008.
- 938 [54] Balakrishnan R, Fitzmaurice G, Kurtenbach G, Singh K. Exploring interactive curve and surface manipulation
939 using a bend and twist sensitive input strip. *Proc. 1999 Symp. Interact. 3D Graph. - SI3D '99*, New York, New
940 York, USA: ACM Press; 1999, p. 111–8. doi:10.1145/300523.300536.
- 941 [55] Benjamin Koh JH, Jeong T, Han S, Li W, Rhode K, Noh Y. Optoelectronic Sensor-based Shape Sensing Approach
942 for Flexible Manipulators. 2019 41st Annu. Int. Conf. IEEE Eng. Med. Biol. Soc., IEEE; 2019, p. 3199–203.
943 doi:10.1109/EMBC.2019.8856882.
- 944 [56] Arkwright JW, Underhill ID, Maunder SA, Blenman N, Szczesniak MM, Wiklendt L, et al. Design of a high-
945 sensor count fibre optic manometry catheter for in-vivo colonic diagnostics. *Opt Express* 2009;17:22423.
946 doi:10.1364/OE.17.022423.
- 947 [57] Merloz P, Troccaz J, Vouaillat H, Vasile C, Tonetti J, Eid A, et al. Fluoroscopy-based navigation system in spine
948 surgery. *Proc Inst Mech Eng Part H J Eng Med* 2007;221:813–20. doi:10.1243/09544119JEIM268.
- 949 [58] Mahesh M. Fluoroscopy: Patient Radiation Exposure Issues. *RadioGraphics* 2001;21:1033–45.
950 doi:10.1148/radiographics.21.4.g01j271033.
- 951 [59] Rivest-Henault D, Sundar H, Cheriet M. Nonrigid 2D/3D Registration of Coronary Artery Models With Live
952 Fluoroscopy for Guidance of Cardiac Interventions. *IEEE Trans Med Imaging* 2012;31:1557–72.
953 doi:10.1109/TMI.2012.2195009.

- 954 [60] Manchikanti L, Cash, McManus, Pampati. Fluoroscopic caudal epidural injections in managing chronic axial low
955 back pain without disc herniation, radiculitis, or facet joint pain. *J Pain Res* 2012;5:381. doi:10.2147/JPR.S35924.
- 956 [61] Ito Y, Sugimoto Y, Tomioka M, Hasegawa Y, Nakago K, Yagata Y. Clinical accuracy of 3D fluoroscopy-assisted
957 cervical pedicle screw insertion: Clinical article. *J Neurosurg Spine* 2008;9:450–3.
958 doi:10.3171/SPL.2008.9.11.450.
- 959 [62] Kahler DM. Image Guidance: Fluoroscopic Navigation. *Clin Orthop Relat Res* 2004;421:70–6.
960 doi:10.1097/01.blo.0000126869.67208.2d.
- 961 [63] Yang C-D, Chen Y-W, Tseng C-S, Ho H-J, Wu C-C, Wang K-W. Non-invasive, fluoroscopy-based, image-guided
962 surgery reduces radiation exposure for vertebral compression fractures: A preliminary survey. *Formos J Surg*
963 2012;45:12–9. doi:10.1016/j.fjs.2011.12.003.
- 964 [64] Tosi D, Schena E, Molardi C, Korganbayev S. Fiber optic sensors for sub-centimeter spatially resolved
965 measurements: Review and biomedical applications. *Opt Fiber Technol* 2018;43:6–19.
966 doi:10.1016/j.yofte.2018.03.007.
- 967 [65] He J, Zhou Z, Jinping O. Optic fiber sensor-based smart bridge cable with functionality of self-sensing. *Mech Syst*
968 *Signal Process* 2013;35:84–94. doi:10.1016/j.ymsp.2012.08.022.
- 969 [66] Roveri N, Carcaterra A, Sestieri A. Real-time monitoring of railway infrastructures using fibre Bragg grating
970 sensors. *Mech Syst Signal Process* 2015;60–61:14–28. doi:10.1016/j.ymsp.2015.01.003.
- 971 [67] Alian H, Konforty S, Ben-Simon U, Klein R, Tur M, Bortman J. Bearing fault detection and fault size estimation
972 using fiber-optic sensors. *Mech Syst Signal Process* 2019;120:392–407. doi:10.1016/j.ymsp.2018.10.035.
- 973 [68] Beisenova A, Issatayeva A, Tosi D, Molardi C. Fiber-Optic Distributed Strain Sensing Needle for Real-Time
974 Guidance in Epidural Anesthesia. *IEEE Sens J* 2018;18:8034–44. doi:10.1109/JSEN.2018.2865220.
- 975 [69] Sultangazin A, Kusmangaliyev J, Aitkulov A, Akilbekova D, Olivero M, Tosi D. Design of a Smartphone Plastic
976 Optical Fiber Chemical Sensor for Hydrogen Sulfide Detection. *IEEE Sens J* 2017;17:6935–40.
977 doi:10.1109/JSEN.2017.2752717.
- 978 [70] Madrigal J, Barrera D, Sales S. Refractive Index and Temperature Sensing Using Inter-Core Crosstalk in Multicore
979 Fibers. *J Light Technol* 2019;37:4703–9. doi:10.1109/JLT.2019.2917629.
- 980 [71] Piestrzyńska M, Dominik M, Kosiel K, Janczuk-Richter M, Szot-Karpińska K, Brzozowska E, et al. Ultrasensitive
981 tantalum oxide nano-coated long-period gratings for detection of various biological targets. *Biosens Bioelectron*
982 2019;133:8–15. doi:10.1016/j.bios.2019.03.006.
- 983 [72] Zhao Y, Zhou X, Li X, Zhang Y. Review on the graphene based optical fiber chemical and biological sensors.
984 *Sensors Actuators B Chem* 2016;231:324–40. doi:10.1016/j.snb.2016.03.026.
- 985 [73] Gertsbakh I. *Measurand and Measurement Errors*. Meas. Theory Eng., Berlin, Heidelberg: Springer Berlin
986 Heidelberg; 2003. doi:10.1007/978-3-662-08583-7_1.
- 987 [74] Pevec S, Donlagić D. Multiparameter fiber-optic sensors: a review. *Opt Eng* 2019;58:1.
988 doi:10.1117/1.OE.58.7.072009.
- 989 [75] Li P, Zhang Z, Zhang J. Simultaneously identifying displacement and strain flexibility using long-gauge fiber optic
990 sensors. *Mech Syst Signal Process* 2019;114:54–67. doi:10.1016/j.ymsp.2018.05.005.
- 991 [76] Zhou Z, Liu W, Huang Y, Wang H, Jianping H, Huang M, et al. Optical fiber Bragg grating sensor assembly for
992 3D strain monitoring and its case study in highway pavement. *Mech Syst Signal Process* 2012;28:36–49.
993 doi:10.1016/j.ymsp.2011.10.003.
- 994 [77] Mieloszyk M, Ostachowicz W. Moisture contamination detection in adhesive bond using embedded FBG sensors.
995 *Mech Syst Signal Process* 2017;84:1–14. doi:10.1016/j.ymsp.2016.07.006.
- 996 [78] Fuhr PL, Kajenski PJ, Kunkel DL, Huston DR. A subcarrier intensity modulated fiber optic sensor for structural
997 vibration measurements. *Mech Syst Signal Process* 1993;7:133–43. doi:10.1006/mssp.1993.1003.
- 998 [79] Griffioen W. Optical fiber mechanical reliability. 1995. doi:10.6100/IR435417.
- 999 [80] Matthewson MJ, Kurkjian CR, Gulati ST. Strength measurement of optical fibers by bending. *J Am Ceram*
1000 *Society* 1986;69:815–21. doi:10.1111/j.1151-2916.1986.tb07366.x.
- 1001 [81] Kurkjian CR, Krause JT, Matthewson MJ. Strength and fatigue of silica optical fibers. *J Light Technol*
1002 1989;7:1360–70. doi:10.1109/50.50715.
- 1003 [82] Glaesemann GS. Advancements in mechanical strength and reliability of optical fibers. *Reliab. Opt. Fibers Opt.*
1004 *Fiber Syst. A Crit. Rev.*, vol. 10295, 1999, p. 1029502. doi:10.1117/12.361072.
- 1005 [83] Florís I, Madrigal J, Sales S, Adam JM, Calderón PA. Experimental study of the influence of FBG length on
1006 optical shape sensor performance. *Opt Lasers Eng* 2020;126:105878. doi:10.1016/j.optlaseng.2019.105878.
- 1007 [84] Florís I, Sales S, Calderón PAPA, Adam JM. Measurement uncertainty of multicore optical fiber sensors used
1008 to sense curvature and bending direction. *Meas J Int Meas Confed* 2019;132:35–46.
1009 doi:10.1016/j.measurement.2018.09.033.
- 1010 [85] Florís I, Calderón PA, Sales S, Adam JM. Effects of core position uncertainty on optical shape sensor accuracy.
1011 *Meas J Int Meas Confed* 2019;139:21–33. doi:10.1016/j.measurement.2019.03.031.
- 1012 [86] Florís I, Madrigal J, Sales S, Calderón PA, Adam JM. Twisting measurement and compensation of optical shape
1013 sensor based on spun multicore fiber. *Mech Syst Signal Process* 2020;140:106700.
1014 doi:10.1016/j.ymsp.2020.106700.
- 1015 [87] Bauchau OA, Craig JI. Euler-Bernoulli beam theory. In: Bauchau OA, Craig JI, editors. *Struct. Anal.*, Dordrecht:
1016 Springer Netherlands; 2009, p. 173–221. doi:10.1007/978-90-481-2516-6_5.
- 1017 [88] Love AEH. *A Treatise on the Mathematical Theory of Elasticity*. vol. 1. 1st ed. Cambridge University Press; 1892.

- 1018 [89] O'Reilly OM. Kirchhoff's Rod Theory. *Model. Nonlinear Probl. Mech. Strings Rods Role Balanc. Laws*, Cham: Springer International Publishing; 2017, p. 187–268. doi:10.1007/978-3-319-50598-5_5.
- 1019 [90] Galloway KC, Chen Y, Templeton E, Rife B, Godage IS, Barth EJ. Fiber Optic Shape Sensing for Soft Robotics. *Soft Robot* 2019;6:671–84. doi:10.1089/soro.2018.0131.
- 1020 [91] Westbrook PS, Feder KS, Kremp T, Taunay TF, Monberg E, Kelliher J, et al. Integrated optical fiber shape sensor modules based on twisted multicore fiber grating arrays. In: Gannot I, editor. *Opt. Fibers Sensors Med. Diagnostics Treat. Appl. XIV*, vol. 8938, 2014, p. 89380H. doi:10.1117/12.2041775.
- 1021 [92] Westbrook PS, Kremp T, Feder KS, Ko W, Monberg EM, Wu H, et al. Continuous Multicore Optical Fiber Grating Arrays for Distributed Sensing Applications. *J Light Technol* 2017;35:1248–52. doi:10.1109/JLT.2017.2661680.
- 1022 [93] Moore JP, Rogge MD. Shape sensing using multi-core fiber optic cable and parametric curve solutions. *Opt Express* 2012;20:2967. doi:10.1364/OE.20.002967.
- 1023 [94] Flockhart GMH, MacPherson WN, Barton JS, Jones JDC, Zhang L, Bennion I. Two-axis bend measurement with Bragg gratings in multicore optical fiber. *Opt Lett* 2003;28:387. doi:10.1364/OL.28.000387.
- 1024 [95] Khan F, Roesthuis RJ, Misra S. Force sensing in continuum manipulators using fiber Bragg grating sensors. *IEEE Int Conf Intell Robot Syst* 2017;2017-Sept:2531–6. doi:10.1109/IROS.2017.8206073.
- 1025 [96] Lenke P, Wendt M, Krebber K, Glötzl R. Highly sensitive fiber optic inclinometer: easy to transport and easy to install. *21st Int. Conf. Opt. Fibre Sensors*, vol. 7753, 2011, p. 775352. doi:10.1117/12.884695.
- 1026 [97] Wang YL, Shi B, Zhang TL, Zhu HH, Jie Q, Sun Q. Introduction to an FBG-based inclinometer and its application to landslide monitoring. *J Civ Struct Heal Monit* 2015;5:645–53. doi:10.1007/s13349-015-0129-4.
- 1027 [98] Roesthuis RJ, Kemp M, van den Dobbelaar JJ, Misra S. Three-Dimensional Needle Shape Reconstruction Using an Array of Fiber Bragg Grating Sensors. *IEEE/ASME Trans Mechatronics* 2014;19:1115–26. doi:10.1109/TMECH.2013.2269836.
- 1028 [99] Liu H, Zhu Z, Zheng Y, Liu B, Xiao F. Experimental study on an FBG strain sensor. *Opt Fiber Technol* 2018;40:144–51. doi:10.1016/j.yofte.2017.09.003.
- 1029 [100] Moon H, Jeong J, Kang S, Kim K, Song Y-W, Kim J. Fiber-Bragg-grating-based ultrathin shape sensors displaying single-channel sweeping for minimally invasive surgery. *Opt Lasers Eng* 2014;59:50–5. doi:10.1016/j.optlaseng.2014.03.005.
- 1030 [101] Villatoro J, Van Newkirk A, Antonio-Lopez E, Zubia J, Schülzgen A, Amezcua-Correa R. Ultrasensitive vector bending sensor based on multicore optical fiber. *Opt Lett* 2016;41:832–5. doi:10.1364/OL.41.000832.
- 1031 [102] MacPherson WN, Silva-Lopez M, Barton JS, Moore AJ, Jones JDC, Zhao D, et al. Tunnel monitoring using multicore fibre displacement sensor. *Meas Sci Technol* 2006;17:1180–5. doi:10.1088/0957-0233/17/5/S41.
- 1032 [103] Fender A, MacPherson WN, Maier RRJ, Barton JS, George DS, Howden RI, et al. Two-axis accelerometer based on multicore fibre Bragg gratings. *IEEE Sens J* 2007;8:66190Q-66190Q – 4. doi:10.1117/12.738411.
- 1033 [104] Lally EM, Reaves M, Horrell E, Klute S, Froggatt ME. Fiber optic shape sensing for monitoring of flexible structures. In: Tomizuka M, Yun C-B, Lynch JP, editors. *Proc. SPIE - Int. Soc. Opt. Eng.*, vol. 8345, 2012, p. 83452Y. doi:10.1117/12.917490.
- 1034 [105] Askins CG, Miller GA, Friebele EJ. Bend and Twist Sensing in a Multiple-Core Optical Fiber. *OFC/NFOEC 2008 - 2008 Conf. Opt. Fiber Commun. Fiber Opt. Eng. Conf.*, IEEE; 2008, p. 1–3. doi:10.1109/OFC.2008.4528404.
- 1035 [106] Collins OM, Vasudev N. The effect of redundancy on measurement. *IEEE Trans Inf Theory* 2001;47:3090–6. doi:10.1109/18.959292.
- 1036 [107] Barrera D, Gasulla I, Sales S. Multipoint Two-Dimensional Curvature Optical Fiber Sensor Based on a Nontwisted Homogeneous Four-Core Fiber. *J Light Technol* 2015;33:2445–50. doi:10.1109/JLT.2014.2366556.
- 1037 [108] Cooper LJ, Webb AS, Gillooly A, Hill M, Read T, Maton P, et al. Design and performance of multicore fiber optimized towards communications and sensing applications. In: Jiang S, Dignonnet MJF, editors. *Proc. SPIE - Int. Soc. Opt. Eng.*, vol. 9359, 2015, p. 93590H. doi:10.1117/12.2076950.
- 1038 [109] Zhao Z, Soto MA, Tang M, Thévenaz L. Distributed shape sensing using Brillouin scattering in multi-core fibers. *Opt Express* 2016;24:25211. doi:10.1364/OE.24.025211.
- 1039 [110] Westbrook PS, Kremp T, Feder KS, Ko W, Monberg EM, Wu H, et al. Performance characteristics of continuously grating multicore sensor fiber. In: Chung Y, Jin W, Lee B, Canning J, Nakamura K, Yuan L, editors. vol. 10323, 2017, p. 103236I. doi:10.1117/12.2263481.
- 1040 [111] Zheng D, Madrigal J, Chen H, Barrera D, Sales S. Multicore fiber-Bragg-grating-based directional curvature sensor interrogated by a broadband source with a sinusoidal spectrum. *Opt Lett* 2017;42:3710. doi:10.1364/OL.42.003710.
- 1041 [112] <https://www.fibercore.com/product/multicore-fiber-n.d>.
- 1042 [113] Zeni L, Picarelli L, Avolio B, Coscetta A, Papa R, Zeni G, et al. Brillouin optical time-domain analysis for geotechnical monitoring. *J Rock Mech Geotech Eng* 2015;7:458–62. doi:10.1016/j.jrmge.2015.01.008.
- 1043 [114] Meltz G, Dunphy JR, Glenn WH, Farina JD, Leonberger FJ. Fiber Optic Temperature And Strain Sensors. In: Verga Scheggi AM, editor., 1987, p. 104. doi:10.1117/12.941093.
- 1044 [115] Zhang S, Bae Lee S, Fang X, Sam Choi S. In-fiber grating sensors. *Opt Lasers Eng* 1999;32:405–18. doi:10.1016/S0143-8166(99)00052-4.
- 1045 [116] Rao Y. Recent progress in applications of in-fiber Bragg grating sensors. *Opt Lasers Eng* 1999;31:297–324. doi:10.1016/S0143-8166(99)00025-1.
- 1046 [117] Ferraro P, De Natale G. On the possible use of optical fiber Bragg gratings as strain sensors for geodynamical monitoring. *Opt Lasers Eng* 2002;37:115–30. doi:10.1016/S0143-8166(01)00141-5.

- 1082 [118] Spirin V., Shlyagin M., Miridonov S., Jiménez FJM, Gutiérrez RML. Fiber Bragg grating sensor for petroleum
1083 hydrocarbon leak detection. *Opt Lasers Eng* 1999;32:497–503. doi:10.1016/S0143-8166(00)00021-X.
- 1084 [119] Botsis J, Humbert L, Colpo F, Giaccari P. Embedded fiber Bragg grating sensor for internal strain measurements
1085 in polymeric materials. *Opt Lasers Eng* 2005;43:491–510. doi:10.1016/j.optlaseng.2004.04.009.
- 1086 [120] Ma Z, Chen X. Fiber Bragg Gratings Sensors for Aircraft Wing Shape Measurement: Recent Applications and
1087 Technical Analysis. *Sensors* 2018;19:55. doi:10.3390/s19010055.
- 1088 [121] Salo J, Korhonen I. Calculated estimate of FBG sensor's suitability for beam vibration and strain measuring.
1089 *Measurement* 2014;47:178–83. doi:10.1016/j.measurement.2013.08.017.
- 1090 [122] Kashyap R. *Fiber Bragg Gratings*. 2nd Editio. Elsevier; 2010.
- 1091 [123] Gribaev AI, Pavlishin I V., Stam AM, Idrisov RF, Varzhel S V., Konnov KA. Laboratory setup for fiber Bragg
1092 gratings inscription based on Talbot interferometer. *Opt Quantum Electron* 2016;48:540. doi:10.1007/s11082-016-
1093 0816-3.
- 1094 [124] Idrisov RF, Varzhel S V., Kulikov A V., Meshkovskiy IK, Rothhardt M, Becker M, et al. Spectral characteristics
1095 of draw-tower step-chirped fiber Bragg gratings. *Opt Laser Technol* 2016;80:112–5.
1096 doi:10.1016/j.optlastec.2016.01.007.
- 1097 [125] Hong C, Yuan Y, Yang Y, Zhang Y, Abro ZA. A simple FBG pressure sensor fabricated using fused deposition
1098 modelling process. *Sensors Actuators, A Phys* 2019;285:269–74. doi:10.1016/j.sna.2018.11.024.
- 1099 [126] Seo H. Monitoring of CFA pile test using three dimensional laser scanning and distributed fiber optic sensors. *Opt*
1100 *Lasers Eng* 2020;130:106089. doi:10.1016/j.optlaseng.2020.106089.
- 1101 [127] Thévenaz L. Review and Progress on Distributed Fibre Sensing. *Opt. Fiber Sensors*, Washington, D.C.: OSA;
1102 2006, p. ThC1. doi:10.1364/OFS.2006.ThC1.
- 1103 [128] Bao X, Chen L. Recent Progress in Distributed Fiber Optic Sensors. *Sensors* 2012;12:8601–39.
1104 doi:10.3390/s120708601.
- 1105 [129] Ding Z, Wang C, Liu K, Jiang J, Yang D, Pan G, et al. Distributed Optical Fiber Sensors Based on Optical
1106 Frequency Domain Reflectometry: A review. *Sensors* 2018;18:1072. doi:10.3390/s18041072.
- 1107 [130] Yuksel K. Rayleigh-based Optical Reflectometry Techniques for Distributed Sensing Applications. 2009 11th Int.
1108 Conf. Transparent Opt. Networks, IEEE; 2009, p. 1–5.
- 1109 [131] Palmieri L. Distributed Optical Fiber Sensing Based on Rayleigh Scattering. *Open Opt J* 2013;7:104–27.
1110 doi:10.2174/1874328501307010104.
- 1111 [132] Loranger S, Gagné M, Lambin-Iezzi V, Kashyap R. Rayleigh scatter based order of magnitude increase in
1112 distributed temperature and strain sensing by simple UV exposure of optical fibre. *Sci Rep* 2015;5:11177.
1113 doi:10.1038/srep11177.
- 1114 [133] Schenato L. A Review of Distributed Fibre Optic Sensors for Geo-Hydrological Applications. *Appl Sci*
1115 2017;7:896. doi:10.3390/app7090896.
- 1116 [134] Thévenaz L. Brillouin distributed time-domain sensing in optical fibers: state of the art and perspectives. *Front*
1117 *Optoelectron China* 2010;3:13–21. doi:10.1007/s12200-009-0086-9.
- 1118 [135] Culverhouse D, Ferahi F, Pannell CN, Jackson DA. Exploitation of stimulated Brillouin scattering as a sensing
1119 mechanism for distributed temperature sensors and as a mean of realizing a tunable microwave generator. *Opt.*
1120 *Fibre Sensors Conf. OFS'89*, Springer Proc. Phys. 44, Berlin: Springer-Verlag; 1989, p. 552.
- 1121 [136] Ishio H, Minowa J, Nosu K. Review and Status of Wavelength-Division-Multiplexing Technology and Its
1122 Application. *J Light Technol* 1984;2:448–63. doi:10.1109/JLT.1984.1073653.
- 1123 [137] Kersey AD, Morey WW. Multiplexed Bragg grating fibre-laser strain-sensor system with mode-locked
1124 interrogation. *Electron Lett* 1993;29:112–4. doi:10.1049/el:19930073.
- 1125 [138] Chen; PC, Sirkis JS. Method and apparatus for determining the shape of a flexible body, US Patent 6256090B1,
1126 2001.
- 1127 [139] Greenaway AH, Burnett JG, Harvey AR, Blanchard PM, Lloyd PA, McBride R, et al. Optical fibre bend sensor,
1128 World Intellectual Property Organization Patent WO1998059219A3.
1129 <https://patents.google.com/patent/WO1998059219A3>, 1998.
- 1130 [140] Greenaway AH, Burnett JG, Harvey AR, McBride PAL, Russell PSJ, Blanchard PM. Optical fiber bend sensor,
1131 US Patent US6389187B1, 2002.
- 1132 [141] Blanchard PM, Burnett JG, Erry GRG, Greenaway AH, Harrison P, Mangan B, et al. Two-dimensional bend
1133 sensing with a single, multi-core optical fibre. *Smart Mater Struct* 2000;9:132–40. doi:10.1088/0964-
1134 1726/9/2/302.
- 1135 [142] Burnett JG, Blanchard PM, Greenaway AH. Optical Fibre-based Vectoral Shape Sensor 2000;36.
- 1136 [143] Gander MJ, MacPherson WN, McBride R, Jones JDC, Zhang L, Bennion I, et al. Bend measurement using Bragg
1137 gratings in multicore fibre. *Electron Lett* 2000;36:2–3.
- 1138 [144] MacPherson WN, Flockhart GMH, Maier RRJ, Barton JS, Jones JDC, Zhao D, et al. Pitch and roll sensing using
1139 fibre Bragg gratings in multicore fibre. *Meas Sci Technol* 2004;15:1642–6. doi:10.1088/0957-0233/15/8/036.
- 1140 [145] Clements GM. Fiber optic sensor for precision 3-D position measurement, US Patent 6888623B2, 2003.
- 1141 [146] Miller GA, Askins CG, Friebele EJ. Shape sensing using distributed fiber optic strain measurements. *Second Eur.*
1142 *Work. Opt. Fibre Sensors*, vol. 5502, 2004, p. 528. doi:10.1117/12.566653.
- 1143 [147] Zhang L, Qian J, Shen L, Zhang Y. FBG sensor devices for spatial shape detection of intelligent colonoscope.
1144 *IEEE Int. Conf. Robot. Autom. 2004. Proceedings. ICRA '04*. 2004, vol. 2004, IEEE; 2004, p. 834-840 Vol.1.
1145 doi:10.1109/ROBOT.2004.1307253.

- 1146 [148] Yi X, Niu F, He J, Fan H. The 3D shape analysis of elastic rod in shape sensing medical robot system. 2010 IEEE
1147 Int. Conf. Robot. Biomimetics, IEEE; 2010, p. 1014–8. doi:10.1109/ROBIO.2010.5723465.
- 1148 [149] Duncan RG, Froggatt ME, Kreger ST, Seeley RJ, Gifford DK, Sang AK, et al. High-accuracy fiber-optic shape
1149 sensing. In: Peters KJ, editor. Phenomena, Technol. Appl. NDE Heal. Monit. 2007, vol. 6530, 2007, p. 65301S.
1150 doi:10.1117/12.720914.
- 1151 [150] Froggatt ME, Duncan RG. Fiber optic position and/or shape sensing based on rayleigh scatter, US Patent
1152 7772541B2, 2010.
- 1153 [151] Moore JP, Rogge MD. Shape Sensing Using a Multi-Core Optical Fiber Having an Arbitrary Initial Shape in the
1154 Presence of Extrinsic Forces, US Patent 8746076B2, 2014.
- 1155 [152] Florís I, Madrigal J, Sales S, Calderón PA, Adam JM. Twisting compensation of optical multicore fiber shape
1156 sensors for flexible medical instruments. In: Gannot I, editor. Opt. Fibers Sensors Med. Diagnostics Treat. Appl.
1157 XX, vol. 1123316, SPIE; 2020, p. 41. doi:10.1117/12.2543783.
- 1158 [153] Xu R, Yurkewich A, Patel R V. Curvature, Torsion, and Force Sensing in Continuum Robots Using Helically
1159 Wrapped FBG Sensors. IEEE Robot Autom Lett 2016;1:1052–9. doi:10.1109/LRA.2016.2530867.
- 1160 [154] Barrera D, Madrigal J, Sales S. Long Period Gratings in Multicore Optical Fibers for Directional Curvature Sensor
1161 Implementation. J Light Technol 2018;36:1063–8. doi:10.1109/JLT.2017.2764951.
- 1162 [155] Zafeiropoulou A, Masoudi A, Zdagkas A, Cooper L, Brambilla G. Curvature sensing with a D-shaped multicore
1163 fibre and Brillouin optical time-domain reflectometry. Opt Express 2020;28:1291. doi:10.1364/OE.383096.
- 1164 [156] Szostkiewicz Ł, Soto MA, Yang Z, Dominguez-Lopez A, Parola I, Markiewicz K, et al. High-resolution distributed
1165 shape sensing using phase-sensitive optical time-domain reflectometry and multicore fibers. Opt Express
1166 2019;27:20763. doi:10.1364/OE.27.020763.
- 1167 [157] Yi X, Qian J, Shen L, Zhang Y, Zhang Z. An Innovative 3D Colonoscope Shape Sensing Sensor Based on FBG
1168 Sensor Array. 2007 Int. Conf. Inf. Acquis., IEEE; 2007, p. 227–32. doi:10.1109/ICIA.2007.4295731.
- 1169 [158] Khan F, Denasi A, Barrera D, Madrigal J, Sales S, Misra S. Multi-Core Optical Fibers With Bragg Gratings as
1170 Shape Sensor for Flexible Medical Instruments. IEEE Sens J 2019;19:5878–84. doi:10.1109/JSEN.2019.2905010.
- 1171 [159] Jäckle S, Eixmann T, Schulz-Hildebrandt H, Hüttmann G, Pätz T. Fiber optical shape sensing of flexible
1172 instruments for endovascular navigation. Int J Comput Assist Radiol Surg 2019;14:2137–45. doi:10.1007/s11548-
1173 019-02059-0.
- 1174 [160] Beisenova A, Issatayeva A, Iordachita I, Blanc W, Molardi C, Tosi D. Distributed fiber optics 3D shape sensing
1175 by means of high scattering NP-doped fibers simultaneous spatial multiplexing. Opt Express 2019;27:22074.
1176 doi:10.1364/OE.27.022074.
- 1177 [161] Parent F, Loranger S, Mandal KK, Iezzi VL, Lapointe J, Boisvert J-S, et al. Enhancement of accuracy in shape
1178 sensing of surgical needles using optical frequency domain reflectometry in optical fibers. Biomed Opt Express
1179 2017;8:2210. doi:10.1364/BOE.8.002210.
- 1180 [162] Chan HM, Allen R. Jr. P. In-situ three-dimensional shape rendering from strain values obtained through optical
1181 fiber sensors, US Patent 8970845B1, 2015.
- 1182 [163] Klute S, Duncan R, Fielder R, Butler G, Mabe J, Sang A, et al. Fiber-Optic Shape Sensing and Distributed Strain
1183 Measurements on a Morphing Chevron. 44th AIAA Aerosp. Sci. Meet. Exhib., Reston, Virginia: American
1184 Institute of Aeronautics and Astronautics; 2006, p. 1–23. doi:10.2514/6.2006-624.
- 1185 [164] Henken KR, Dankelman J, Van Den Dobbela JJ, Cheng LK, Van Der Heiden MS. Error Analysis of FBG-
1186 Based Shape Sensors for Medical Needle Tracking. IEEE/ASME Trans Mechatronics 2014;19:1523–31.
1187 doi:10.1109/TMECH.2013.2287764.
- 1188 [165] van der Heiden MS, Henken KR, Chen LK, van den Bosch BG, van den Braber R, Dankelman J, et al. Accurate
1189 and efficient fiber optical shape sensor for MRI compatible minimally invasive instruments. In: Mazuray L,
1190 Wartmann R, Wood AP, de la Fuente MC, Tissot J-LM, Raynor JM, et al., editors. Opt. Syst. Des. 2012, vol. 8550,
1191 2012, p. 85500L. doi:10.1117/12.981141.
- 1192 [166] Jibson RW. Methods for assessing the stability of slopes during earthquakes—A retrospective. Eng Geol
1193 2011;122:43–50. doi:10.1016/j.enggeo.2010.09.017.
- 1194 [167] Shanmugam G, Wang Y. The landslide problem. J Palaeogeogr 2015;4:109–66.
1195 doi:10.3724/SP.J.1261.2015.00071.
- 1196 [168] Simeoni L, Mongiovì L. Inclinometer Monitoring of the Castelrotto Landslide in Italy. J Geotech
1197 Geoenvironmental Eng 2007;133:653–66. doi:10.1061/(ASCE)1090-0241(2007)133:6(653).
- 1198 [169] Miller GA, Askins CG, Cranch GA. Interferometric interrogation of a multicore fiber, two-axis inclinometer. In:
1199 Jones JDC, editor. 20th Int. Conf. Opt. Fibre Sensors, vol. 7503, 2009, p. 75032R. doi:10.1117/12.835386.
- 1200 [170] Zheng D, Liu Z, Florís I, Sales S. Temperature-insensitive 2D inclinometer based on pendulum-assisted fiber
1201 Bragg gratings. In: Kalli K, Brambilla G, O’Keeffe SO, editors. Seventh Eur. Work. Opt. Fibre Sensors, vol.
1202 1119905, SPIE; 2019, p. 17. doi:10.1117/12.2539286.
- 1203 [171] Miller GA. Fabrication of a Multifiber Optical Inclinometer. IEEE Photonics Technol Lett 2015;27:1289–92.
1204 doi:10.1109/LPT.2015.2420853.
- 1205 [172] Li J, Correia R, Chehura E, Staines S, James SW, Tatam RP. A fibre Bragg grating-based inclinometer system for
1206 ground movement measurement. In: Santos JL, Culshaw B, López-Higuera JM, MacPherson WN, editors. Proc.
1207 SPIE - Int. Soc. Opt. Eng., vol. 7653, 2010, p. 765314. doi:10.1117/12.866334.
- 1208 [173] MacPherson WN, Silva-Lopez M, Barton JS, Moore AJ, Jones JDC, Zhao D, et al. Tunnel monitoring using
1209 multicore fiber displacement sensor. vol. 5855, 2005, p. 274. doi:10.1117/12.623992.

- 1210 [174] Nair A, Cai CS. Acoustic emission monitoring of bridges: Review and case studies. *Eng Struct* 2010;32:1704–14.
1211 doi:10.1016/j.engstruct.2010.02.020.
- 1212 [175] Chen Z, Zhou X, Wang X, Dong L, Qian Y. Deployment of a Smart Structural Health Monitoring System for
1213 Long-Span Arch Bridges: A Review and a Case Study. *Sensors* 2017;17:2151. doi:10.3390/s17092151.
- 1214 [176] Kang D, Chung W. Integrated monitoring scheme for a maglev guideway using multiplexed FBG sensor arrays.
1215 *NDT E Int* 2009;42:260–6. doi:10.1016/j.ndteint.2008.11.001.
- 1216 [177] Uva G, Porco F, Fiore A, Porco G. Structural monitoring using fiber optic sensors of a pre-stressed concrete viaduct
1217 during construction phases. *Case Stud Nondestruct Test Eval* 2014;2:27–37. doi:10.1016/j.csdnt.2014.06.002.
- 1218 [178] Uva G, Raffaele D, Porco F, Fiore A, Porco G. Bridge monitoring by fiber optic deformation sensors. *Proc. Sixth*
1219 *Int. Conf. Bridg. Maintenance, Saf. Manag.*, 2012, p. 3911–8. doi:10.1201/b12352-583.
- 1220 [179] Porco F, Fiore A, Porco G, Uva G. Monitoring and safety for prestressed bridge girders by SOFO sensors. *J Civ*
1221 *Struct Heal Monit* 2013;3:3–18. doi:10.1007/s13349-012-0029-9.
- 1222 [180] Kissinger T, Chehura E, Staines SE, James SW, Tatam RP. Dynamic Fiber-Optic Shape Sensing Using Fiber
1223 Segment Interferometry. *J Light Technol* 2018;36:917–25. doi:10.1109/JLT.2017.2750759.
- 1224 [181] Wymore ML, Van Dam JE, Ceylan H, Qiao D. A survey of health monitoring systems for wind turbines. *Renew*
1225 *Sustain Energy Rev* 2015;52:976–90. doi:10.1016/j.rser.2015.07.110.
- 1226 [182] Bang H-J, Kim H-I, Lee K-S. Measurement of strain and bending deflection of a wind turbine tower using arrayed
1227 FBG sensors. *Int J Precis Eng Manuf* 2012;13:2121–6. doi:10.1007/s12541-012-0281-2.
- 1228 [183] Hu W-H, Thöns S, Rohrmann RG, Said S, Rucker W. Vibration-based structural health monitoring of a wind
1229 turbine system Part II: Environmental/operational effects on dynamic properties. *Eng Struct* 2015;89:273–90.
1230 doi:10.1016/j.engstruct.2014.12.035.
- 1231 [184] Barrera D, Madrigal J, Delepine-Lesoille S, Sales S. Multicore optical fiber shape sensors suitable for use under
1232 gamma radiation. *Opt Express* 2019;27:29026. doi:10.1364/OE.27.029026.
- 1233 [185] Gherlone M, Cerracchio P, Mattone M. Shape sensing methods: Review and experimental comparison on a wing-
1234 shaped plate. *Prog Aersp Sci* 2018;99:14–26. doi:10.1016/j.paerosci.2018.04.001.
- 1235 [186] Nicolas M, Sullivan R, Richards W. Large Scale Applications Using FBG Sensors: Determination of In-Flight
1236 Loads and Shape of a Composite Aircraft Wing. *Aerospace* 2016;3:18. doi:10.3390/aerospace3030018.
- 1237 [187] Freydn M, Rattner MK, Raveh DE, Kressel I, Davidi R, Tur M. Fiber-Optics-Based Aeroelastic Shape Sensing.
1238 *AIAA J* 2019;57:5094–103. doi:10.2514/1.J057944.
- 1239 [188] Trivedi D, Rahn CD, Kier WM, Walker ID. Soft robotics: Biological inspiration, state of the art, and future
1240 research. *Appl Bionics Biomech* 2008;5:99–117. doi:10.1080/11762320802557865.
- 1241 [189] Kim S, Laschi C, Trimmer B. Soft robotics: a bioinspired evolution in robotics. *Trends Biotechnol* 2013;31:287–
1242 94. doi:10.1016/j.tibtech.2013.03.002.
- 1243 [190] Cianchetti M, Laschi C, Menciassi A, Dario P. Biomedical applications of soft robotics. *Nat Rev Mater*
1244 2018;3:143–53. doi:10.1038/s41578-018-0022-y.
- 1245 [191] Wang H, Zhang R, Chen W, Liang X, Pfeifer R. Shape Detection Algorithm for Soft Manipulator Based on Fiber
1246 Bragg Gratings. *IEEE/ASME Trans Mechatronics* 2016;21:2977–82. doi:10.1109/TMECH.2016.2606491.
- 1247 [192] Li T, Qiu L, Ren H. Distributed Curvature Sensing and Shape Reconstruction for Soft Manipulators With Irregular
1248 Cross Sections Based on Parallel Dual-FBG Arrays. *IEEE/ASME Trans Mechatronics* 2020;25:406–17.
1249 doi:10.1109/TMECH.2019.2949151.
- 1250 [193] Shi C, Luo X, Qi P, Li T, Song S, Najdovski Z, et al. Shape Sensing Techniques for Continuum Robots in
1251 Minimally Invasive Surgery: A Survey. *IEEE Trans Biomed Eng* 2017;64:1665–78.
1252 doi:10.1109/TBME.2016.2622361.
- 1253 [194] Baura GD. Catheters, Bare Metal Stents, and Synthetic Grafts. *Med. Device Technol.*, vol. 1999, Elsevier; 2012,
1254 p. 165–92. doi:10.1016/B978-0-12-374976-5.00008-6.
- 1255 [195] K. Mandal K, Parent F, Martel S, Kashyap R, Kadoury S. Calibration of a needle tracking device with fiber Bragg
1256 grating sensors. In: Webster RJ, Yaniv ZR, editors. *Med. Imaging 2015 Image-Guided Proced. Robot. Interv.*
1257 *Model.*, vol. 9415, 2015, p. 94150X. doi:10.1117/12.2081198.
- 1258 [196] Henken K, Van Gerwen D, Dankelman J, Van Den Dobbelsteen J. Accuracy of needle position measurements
1259 using fiber Bragg gratings. *Minim Invasive Ther Allied Technol* 2012;21:408–14.
1260 doi:10.3109/13645706.2012.666251.
- 1261 [197] Park Y, Elayaperumal S, Daniel B, Ryu SC, Shin M, Savall J, et al. Real-Time Estimation of 3-D Needle Shape
1262 and Deflection for MRI-Guided Interventions. *IEEE/ASME Trans Mechatronics* 2010;15:906–15.
1263 doi:10.1109/TMECH.2010.2080360.
- 1264 [198] Floris I, Madrigal J, Sales S, Adam JM, Calderón PA. Experimental study of the influence of FBG length on
1265 optical shape sensor performance. *Asia Commun. Photonics Conf.*, IEEE; 2019.
- 1266 [199] Jäckle S, Strehlow J, Heldmann S. Shape Sensing with Fiber Bragg Grating Sensors. In: Handels H, Deserno TM,
1267 Maier A, Maier-Hein KH, Palm C, Tolxdorff T, editors. *Bild. für die Medizin* 2019, Wiesbaden: Springer
1268 Fachmedien Wiesbaden; 2019, p. 258–63. doi:10.1007/978-3-658-25326-4_58.
- 1269 [200] Floris I, Adam JM, Calderón PA, Sales S. Measurement uncertainty of 7-core multicore fiber shape sensors. In:
1270 Kalli K, Brambilla G, O’Keeffe SO, editors. *Seventh Eur. Work. Opt. Fibre Sensors, SPIE*; 2019, p. 22.
1271 doi:10.1117/12.2539421.
- 1272